CZECH UNIVERSITY OF LIFE SCIENCES – PRAGUE

FACULTY OF ENVIRONMENTAL SCIENCES

BACHELOR THESIS

2023 Author: Sofiya Tumanova

CZECH UNIVERSITY OF LIFE SCIENCES – PRAGUE

FACULTY OF ENVIRONMENTAL SCIENCES

Study Program: Geographic Information Systems and Remote Sensing in Environmental Science

BACHELOR THESIS

Monitoring of Plastic Debris in the Marine Ecosystem with Remote Sensing

Bachelor Thesis Supervisor: Ing. DAVID MORAVEC, Ph.D.

Author: SOFIYA TUMANOVA

2023

CZECH UNIVERSITY OF LIFE SCIENCES PRAGUE

Faculty of Environmental Sciences

BACHELOR THESIS ASSIGNMENT

Sofiya Tumanova

Geographic Information Systems and Remote Rensing in Environmental Sciences

Thesis title

Monitoring of Plastic Debris in the Marine Ecosystem with Remote Sensing

---

Objectives of thesis

Plastic litter poses a significant threat to the marine ecosystem. Modern technological advancements in remote sensing propose effective and sustainable solutions to monitor plastic litter on a large spatial scale. This thesis aims to perform an in-depth literature review, comparing existing methods and solutions for detecting ocean plastic debris.

Additionally, the goal will involve using freely available remote sensing data to find an algorithm for optimal plastic detection. Furthermore, using a spectroradiometer, this study will create and analyze the spectral properties of plastic samples commonly found in marine environments. Spectral data of plastics will allow a better understanding of the detection and monitoring of floating plastics in the marine ecosystem.

Methodology

This study will involve using the SNAP remote sensing software to analyze the spectral properties of floating plastics using freely available in-situ data from previously conducted experiments. Different bands and indices of the Sentinel-2 satellite data will be analyzed and compared to obtain an optimal result for floating plastic recognition. Reflectance data of pixels from plastic targets and various water depths will be extracted from the experimental sites. The extracted values will be used to create a formula to best detect floating plastics apart from other materials in the water. A spectroradiometer will record and analyze the spectral properties of plastic samples commonly found in floating marine debris. A spectral curve will be generated and analyzed to obtain trends and patterns of plastics' spectral behavior.

The proposed extent of the thesis

30 pages

Keywords

marine litter, remote sensing, plastic pollution, plastic detection

---

Recommended information sources

Basu, B., Sannigrahi, S., Basu, A. S. S., Pilla, F., 2021: Development of Novel Classification Algorithms for Detection of Floating Plastic Debris in Coastal Waterbodies Using Multispectral Sentinel-2 Remote Sensing Imagery, (on-line): https://www.researchgate.net/publication/351009897_Development_of_Novel_Classification_Algorithms_fo 2_Remote_Sensing_Imagery

Biermann, L., Clewley, D., Martinez-Vicente, V., Topouzelis, K., 2020: Finding plastic patches in coastal waters using optical satellite data. Nature News. (on-line) https://www.nature.com/articles/s41598-020-62298-z .

Guffogg, J., Blades, S., Soto-Berelov, M., Bellman, C. J., Skidmore, A. K., Jones, S. D., 2021: Quantifying marine plastic debris in a beach environment using spectral analysis. MDPI, (on-line): https://www.mdpi.com/2072-4292/13/22/4548 .

Themistocleous, K., Papoutsa, C., Michaelides, S., & Hadjimitsis, D., 2020: Investigating detection of floating plastic litter from space using sentinel-2 imagery. MDPI. (on-line) https://www.mdpi.com/2072-4292/12/16/2648 .

Topouzelis, K., Papakonstantinou, A., Shungudzemwoyo P. Garaba,. 2019: Detection of floating plastics from satellite and unmanned aerial systems (Plastic Litter Project 2018), International Journal of Applied Earth Observation and Geoinformation, Volume 79, Pages 175-183, ISSN 1569-8432, (on-line): https://doi.org/10.1016/j.jag.2019.03.011 .

Expected date of thesis defence

2022/23 SS – FES

The Bachelor Thesis Supervisor

Ing. David Moravec, Ph.D.

Supervising department

Department of Spatial Sciences

Electronic approval: 28. 2. 2023

doc. Ing. Petra Šímová, Ph.D.

Head of department

Electronic approval: 1. 3. 2023

prof. RNDr. Vladimír Bejček, CSc.

Dean

Prague on 26. 03. 2023

AUTHOR'S DECLARATION

I hereby declare that I have independently elaborated the bachelor/final thesis with the topic of: ***Monitoring of Plastic Debris in the Marine Ecosystem with Remote Sensing*** *and that I have cited all of the information sources that I used in the thesis as listed at the end of the thesis in the list of used information sources. I am aware that my bachelor/final thesis is subject to Act No. 121/2000 Coll., on copyright, on rights related to copyright and on amendments of certain acts, as amended by later regulations, particularly the provisions of Section 35(3) of the act on the use of the thesis. I am aware that by submitting the bachelor/final thesis I agree with its publication under Act No. 111/1998 Coll., on universities and on the change and amendments of certain acts, as amended, regardless of the result of its defense. With my own signature, I also declare that the electronic version is identical to the printed version and the data stated in the thesis has been processed in relation to the GDPR.*

In: *Prague, Czech Republic* Date: *14 March, 2023*

.....

ACKNOWLEDGEMENTS

I would like to thank my thesis supervisor David Moravec for his patience, motivation, and guidance throughout the process of writing this thesis.

Abstract

Ongoing technological advancements in the field of remote sensing propose a sustainable and efficient solution to tackling the global plastic pollution problem. Although new studies are emerging, the use of remote sensing for the purpose of marine litter detection is a novel topic, with limited availability of in-situ data for accurate and extensive measurements. This study compares the existing methodologies performed in recent years to detect, analyze, and monitor floating plastic from space. Furthermore, this study utilizes freely-available Sentinel-2 remote sensing data containing the presence of plastic in the ocean, to test the effectivity of the existing 'Random Forest' algorithm to detect floating plastic debris. The in-situ data used in this study was acquired from previously conducted experiments, where artificial plastic targets of various sizes were set up to simulate plastic debris in the oceans. Using Sentinel-2's Multispectral Instrument and an open-source atmospheric corrector, pixel values corresponding to plastic, as well as various water depths were extracted and inputted into the algorithm for optimal plastic detection. The Random Forest algorithm tested in this study showed promising results, being able to detect plastic pixels with a 91.5% accuracy. Furthermore, to better understand the spectral behavior of plastic, commonly occurring marine plastic samples were gathered and analyzed using a spectroradiometer, and a plastic spectral graph was generated.

Keywords: marine litter, plastic pollution, plastic detection, remote sensing

Abstrakt

Technologický pokrok v oblasti dálkového průzkumu Země přináší dlouhodobě udržitelné a účinné řešení celosvětového problému sledování znečištění oceánu plasty. I přes stále nové studie je však využití dálkového průzkumu Země pro účely detekce plovoucího odpadu v mořích novým tématem a má jen omezenou dostupnost in situ měření pro přesné a rozsáhlé experimenty. Tato práce porovnává nejnovější metodiky k detekci, analýze a monitorování plovoucích plastů pomocí satelitního průzkumu Země. K tomu tato práce využívá volně dostupná data ze satelitu Sentinel-2 pro testování účinnosti stávajících algoritmů "náhodného lesa" pro detekci plovoucího plastového odpadu. In-situ data použitá v této studii byla získána díky dříve provedeným experimentům, kde byly zřízeny umělé plastové cíle různých velikostí, aby simulovaly plastové úlomky plovoucí v oceánech. Pomocí multispektrálního senzoru družice Sentinel-2 a volně dostupné neuronové sítě C2RCC byly extrahovány hodnoty pixelů odpovídající plastům, stejně jako pixely odpovítající různým hloubkám vody, a byl vytvořen algoritmus pro optimální detekci plastů. Algoritmus Random Forest testovaný v této studii ukázal slibné výsledky a byl schopen detekovat plastové pixely s přesností 91,5 %. Dále pro lepší pochopení spektrálního chování plastů byly shromážděny a analyzovány běžně se vyskytující vzorky mořského plastu pomocí spektroradiometru a byla vytvořena knihovna spektrálních příznaků.

Klíčová slova: plovoucí odpad, znečištění plasty, detekce plastů, dálkový průzkum Země

Table of Contents

1. Introduction

Plastic is an organic polymer made from a variety of natural elements such as hydrogen, oxygen, nitrogen, and carbon through the process of polymerization (monomers joining together to form a polymer) (Brown, 2022). It's low cost, durability, light weight, and moldable nature, made this material so widely used in the modern world, amounting to a total of 322 million tons in 2015 (Piao Ma et al. 2019). Plastic's versatility contributed to its use in almost every aspect of human lives, ranging from food packaging, clothing items, transportation vehicles, infrastructure, medical equipment, and much more (Johnson, 2019). Scientists estimate that around 12.7 million tons of plastic enters the marine ecosystem every year, after which it begins breaking down into smaller particles due to the effects of wind, sunlight, and water (Price, 2019). The plastic particles continue to degrade into smaller and smaller fragments, also known as 'microplastics' which are smaller than 5 millimeters in diameter (defined by the National Oceanic and Atmospheric Administration (NOAA)) (Piao Ma et al. 2019). Microplastics pose a considerable threat when they are ingested by various aquatic organisms such as plankton or fish and continue their way through the aquatic food web (Wagner et al. 2014). These small fragments cause direct physical harm to aquatic organisms by leaking toxins, contaminants, and other harmful plastic additives into the organism's system. Whether added through manufacturing, or absorbed through the environment, plastics contain additives such as flame-retardants, pigments, fillers, and UV stabilizers that contain hazardous substances, and disrupt the endocrine system of aquatic organisms (GESAMP, 2019). Additionally, microplastics have a tendency to attract hydrophobic persistent organic pollutants (man-made chemicals) which bind to floating plastics in the water (Wright, 2013).

Numerous studies have been conducted to find a solution to the global plastic pollution problem, and have shown that remote sensing systems such as Unmanned Aerial Vehicles (UAVs) and satellites can potentially be very effective in identifying and monitoring floating ocean plastics. Remote sensing involves acquiring information about materials on Earth without making direct contact with them. This is done by various sensors installed aboard satellites and aircrafts, which are able to record and distinguish the energy emitted from objects on Earth. Floating plastics are usually found within 0.5

meters of the water surface, thus can be observed by satellites (Kooi et al. 2016). The size and shape of plastic litter greatly varies and affects how the plastics behave, transport, and degrade in the marine environment. GESAMP (2019) took the measure to classify marine plastics into five distinct categories according to size: Mega (>1 m), Macro (25 – 1000 mm), Meso (5 – 25 mm), Micro (<5 mm), Nano (<1 μm). The categories help researches choose appropriate measures when considering methods of plastic detection and monitoring. Large observation programs such as Copernicus (run by the European Space Agency) have conducted experiments to test the effectivity of satellites in plastic litter monitoring (Topouzelis, 2019). Satellites are known to have a large spatial coverage, meaning they can provide extensive information about the land and ocean surface, which makes them an effective tool in Earth observations. They contain various sensors that are able to measure the energy emitted from different materials on Earth, thus allowing scientists to identify substances based on their radiative properties (Brown, 2005). Plastic's chemical properties can be identified using the near infra-red (NIR) and shortwave infra-red (SWIR) parts of the electromagnetic spectrum, which earth observation satellites can distinguish. Using knowledge about plastic's spectral properties allowed researchers to successfully detect large plastic items such as fishing nets in the "Great Pacific Garbage Patch" (Guffogg, 2021). However, detecting plastics based on their spectral properties alone, can often be challenging. In the natural environment, plastic is often mixed with other organic substances such as seaweed, algae, and seafoam. Naturally these materials have a unique spectral reflectance that differ to those of plastic and can interfere with its signal. Additionally, effects of the atmosphere such as cloud cover can have a strong impact on the signal that is being received by the satellite (Moshtaghi, 2021), making plastic, and other materials hard to distinguish from space.

2. Objectives of the thesis

Detection of floating plastic is essential before it begins breaking down and entering the marine ecosystem through ingestion of aquatic organisms, integrating itself into the marine food web. Modern technological advancements in the field of remote sensing and unmanned aerial systems (UAS) present effective and sustainable approaches to detect, monitor, and analyze marine plastic pollution. This study aims to investigate

the issues in relation to marine plastic detection, as well as to compare existing methods of plastic detection using remote sensing systems and UAS through literature review. Furthermore, this study aims to extract the spectral properties of plastic by gathering commonly occurring marine plastic samples, and analyzing them using a spectroradiometer. To better understand the spectral behavior of plastic, a spectral graph will be generated using the results of the spectroradiometer analysis. Additionally, freely available remote sensing images containing in-situ data of floating plastic, will be collected and analyzed with the aim to create an algorithm that will distinguish plastic apart from other pixels. Various satellite bands and band combinations (indices) will be tested to create an optimal combination for detecting floating plastic debris. Details about freely available remote sensing images containing in-situ data of plastic, as well as the algorithms and processes that were conducted are described in detail in the Methodology Section 5.1-5.2. Information about the type of plastic samples gathered for the spectroradiometer analysis, as well as the methodology used, can be found in Section 5.3 of this study.

3. Review of Related Literature

Tackling plastic pollution in the marine ecosystem, is now one of the primary goals of many researchers. Numerous studies have been conducted to try and find the most optimal way to detect plastic apart from other naturally occurring materials such as seaweed, sea foam, and other marine debris. Some of the earliest studies in marine plastic detection began in the 1970s where plastic, and other man-made debris, were visually monitored by scientific personnel aboard ships (Venrick et al. 1973). Modern technological advancements in remote sensing and unmanned aerial vehicles, allowed scientists to perform far more in-depth analysis on marine plastic litter. A project called "Plastic Litter Project 2018: Drone mapping and Satellite Testing for Marine Plastic on the Aegean Sea" (PLP18) was the first project conducted to test the reliability of UAS and open access satellite data in detection on marine plastic. The aim of this project was to use the Copernicus Sentinel-2 satellite to track man-made plastic targets from space, and furthermore to use UAS to enhance the geo-referencing of the coarse resolution of data obtained from the satellite. On the 6th and 7th of June 2018, Topouzelis et al. (2019)

deployed three man-made plastic targets composed of plastic bottles, plastic bags, and plastic fishing nets, close to the shore of Tsamakia Beach in Mytilene, Greece. The targets were designed to match the Sentinel-2 spatial resolution, thus were 10 x 10 m in area, and were positioned at least 30 meters from the coastline. The S900 UAV was used to collect very fine resolution imagery with the accuracy of 3-5 centimeters on June 7, 2018, in the same area. The flight altitude of the UAV was set to 100 meters above sea level, and the drone captured 2846 images in total, which were converted into true color orthorectified images. The process of orthorectification ensures that geometric errors such as sensor orientation, earth curvature, and optical distortions are removed (Esri Insider, 2016). It also ensures that the images taken from the UAV have a known coordinate system, that can be later matched with the images of the Sentinel 2 satellite. They concluded that plastic showed high reflectance in the NIR waveband (842 nm), meanwhile water had a low reflectance in this waveband. Water strongly absorbs light in the NIR and SWIR parts of the electromagnetic spectrum (Kou et. al 1993) thus making plastic materials stand out apart from water.

The date of the experiment was picked according to the day that the Sentinel-2 satellite would fly above the target area (June 7, 2018). Similarly to images taken from S900-UAS, the Sentinel-2 satellite was successful at detecting the three plastic targets in the true color composite; where red = 665 nanometers, green = 560 nanometers, and blue = 490 nanometers. The imagery from S900-UAV and Sentinel-2 was compared based on the spectral reflectance of the plastic targets in both images. The UAV images with a high resolution of 3 centimeters were used to improve the geo-referencing of the Sentinel-2 images, which had a 10 meter resolution. Topouzelis et al. (2019), demonstrated for the first time, how remote sensing and UAVs can be used in the detection of floating marine plastics. The focus was purely on identifying floating plastics using freely available satellite data, as well as using unmanned aerial systems with high geospatial resolution to improve the geo-referencing of the satellite images.

Furthermore, Topouzelis et al. (2019) explored the use of Synthetic Aperture Radar (SAR) aboard the Sentinel-1 satellite to monitor plastic litter. Similarly, to the previous images collected by Sentinel-2 MSI sensor and the S900-UAV, the SAR images were

obtained on the 7th of June 2018 in the same location. Unlike the MSI sensor used for optical imagery on Sentinel-2, SAR is an active sensor, which has the capability to transmit microwave signals to the Earth, and record their backscatter. This allows it to operate in the dark, as well as areas with heavy cloud cover, or rain (Laurencelle, 2022). The study concluded that using the Sentinel-1 radar did not lead to accurate detection of all three plastic targets. It was only able to identify the target consisting of plastic bottles, because the backscatter produced from fishing nets and plastic bags was too low meaning the targets would not be distinguishable from water.

Topouzelis et al. (2019) highlighted the importance of taking in-situ measurements of other commonly found materials in marine ecosystems like algae, suspended sediments, as well as other organic matter, as this could improve the accuracy of plastic detection. This study did not explore scenarios where plastic is integrated with other naturally occurring materials in marine debris, however, this issue was further examined in another study by Biermann et al., 2020.

Biermann et al., (2020) conducted a study with the aim to detect macroplastics (plastics greater than 5 mm in diameter) using the Multi-Spectral Instrument (MSI) sensor located aboard the Sentinel-2 satellite. Furthermore, their study aimed to investigate the spectral properties of various materials integrated with marine debris, and classify macroplastics apart from these materials on a sub-pixel scale. Using reflectance patterns from 10 bands of the Sentinel-2 MSI sensor, they were able to create spectral signatures of various materials such as seaweed, timber, seawater, seafoam, and macroplastics, all of which commonly make up large patches of marine debris. Knowing that water absorbs light in the near infrared (NIR) spectrum, they were able to distinguish plastic, as it shows a reflectance peak in the NIR (central wavelength of 842 nanometers). Their study found that seaweed, unlike plastic, reflects light in the green (560 nm) and red edge (700 – 780nm) bands. They examined other materials and composed a graph of their unique spectral signatures (Figure 3.1)

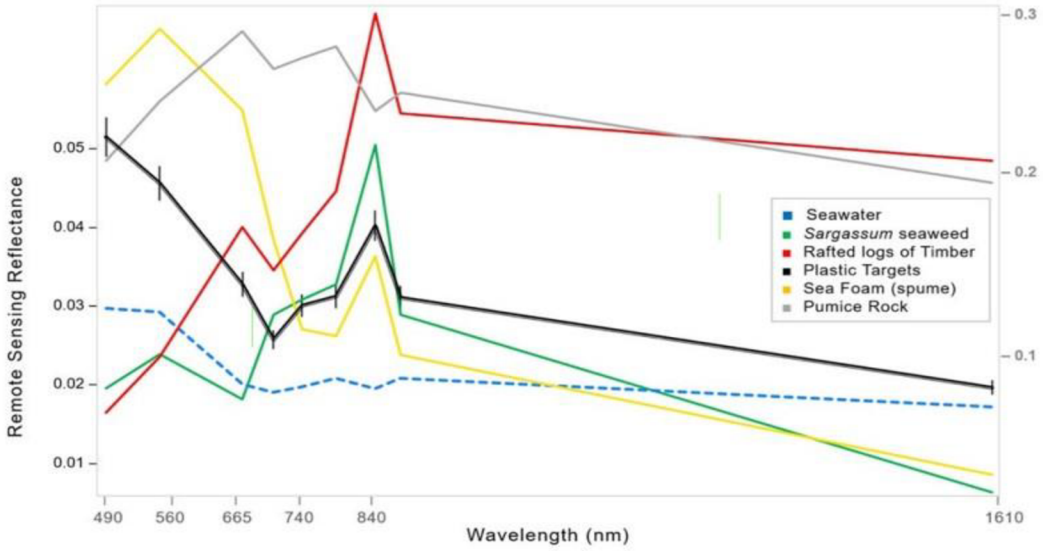

Figure 3.1 *Spectral signatures of different materials commonly found in marine debris. The x-axis depicts the range of Sentinel-2 MSI bands from visible blue light (490 nm) to short-wave infrared light (1610 nm). The left y-axis depicts spectral reflectance of seawater, seaweed, sea foam and plastic, meanwhile the right y-axis depicts the spectral reflectance of timber and pumice. Figure by Biermann et al. 2020 (https://www.nature.com/articles/s41598-020-62298-z)*

Moreover, Biermann et al. (2020) developed a novel index, known as the Floating Debris Index (FDI), which was based on the Floating Algae Index (FAI) tested and analyzed by Hu et al. (2015). FAI utilized the multi-spectral satellite sensors such as the Moderate Resolution Imaging Spectroradiometer (MODIS). The novel Floating Debris Index was applied on plastic targets deployed in Mytilene, Greece in an experiment conducted by Topouzelis et. al (2019). The FDI was found to be successful in detecting floating macroplastics within mixed debris when using it with known spectral signatures of different materials. The FDI works in a way where instead of the red band (used in FAI) the MSI Red Edge (RE) band is used. The FDI formula is as follows:

$$
\begin{aligned}
FDI &= R_{rs,NIR} - R'_{rs,NIR} \\
R'_{rs,NIR} &= R_{rs,RE2} + (R_{rs,SWIR1} - R_{rs,RE2}) \times \frac{(\lambda_{NIR} - \lambda_{RED})}{(\lambda_{SWIR1} - \lambda_{RED})} \times 10
\end{aligned}
$$

Figure 3.2*: Floating Debris Index formula developed by Biermann et. al 2020 showing the use of near infrared (NIR), red edge 2 (RE2), short wave infrared 1 (SWIR1), and red bands in identifying floating plastic debris. Formula developed by Biermann et al. 2020 : (https://www.nature.com/articles/s41598-020-62298-z)*

The Normalized Difference Vegetation Index (NDVI) was applied in this study as well, to distinguish vegetation apart from other materials composing floating debris. According to Hu (2009), vegetation such as algae, present in the aquatic ecosystem, has an increase in reflectance at around 700 nanometers. The NDVI index works by identifying the difference between the red and the near infrared bands allowing for the detection of photosynthetic activity, thus distinguishing vegetation (Biermann et al. 2020). The study concludes that using the NDVI alone can be used to distinguish plastics from seawater, seaweed, timber, and sea foam. When FDI was used alone the ranges of materials found in marine debris were larger, depending on how much of a given pixel was filled with the material (Figure 3.3). Using the two indices (NDVI and FDI) together showed distinct clustering of individual materials (Figure 3.4). The study tested the combination of using the FDI together with the created spectral signature of plastic on five different locations where floating macroplastics were likely to be found: Scotland, Ghana, South Africa, Vietnam, and Canada. The study concluded that the application of FDI with the spectral signature of plastic, on Sentinel-2's Multispectral Instrument was successful at detecting the plastic materials on a sub-pixel scale (less than 10 x 10 meters), as long as the plastic covered at least 30 – 55% of the pixel.

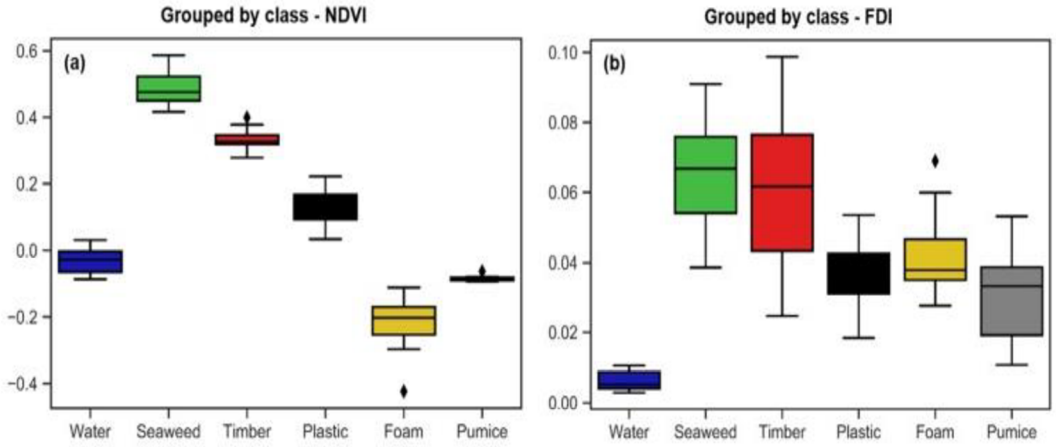

Figure 3.3 *Graphs depicting the distribution of values in different categories of materials: water, seaweed, timber, plastic, foam, pumice. Classifying materials by NDVI alone (left) allows materials to form distinct ranges that do not overlap with plastic. Using FDI alone (right) gives more overlap in the ranges, as well as higher values depending on the amount of materials present in a given pixel. Figure by Biermann et. al 2020: (https://www.nature.com/articles/s41598-020-62298-z)*

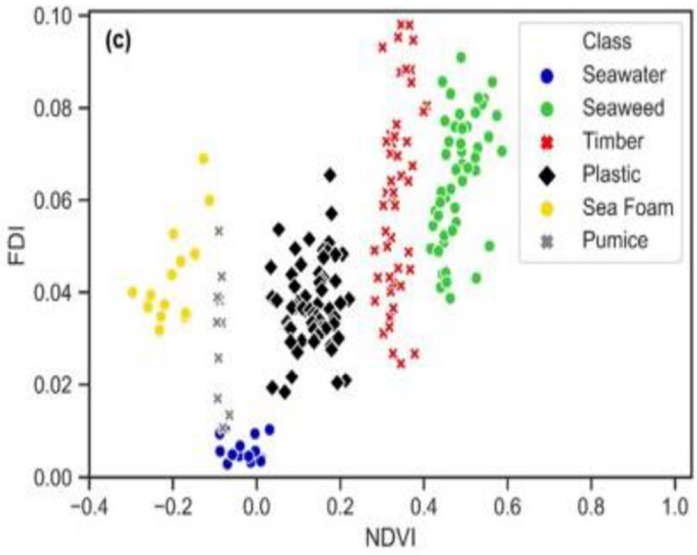

***Figure 3.4**: Graph depicting the distribution of values of different materials (seawater, seaweed, timber, plastic, sea foam, and pumice), when NDVI and FDI are applied together. Materials depicted in a 2-variable space (FDI and NDVI) demonstrates clear clustering within individual materials. Figure by Biermann et al. 2020: (https://www.nature.com/articles/s41598-020-62298-z)*

Another study done by Basu et al. (2021) aimed to identify floating plastic debris by developing novel classification algorithms and applying it on freely available multispectral Sentinel-2 remote sensing imagery. The study considered using in-situ data of plastic in the ocean by selecting two sites where plastic targets were deployed in previous experiments. The two locations of existing plastic targets were Limassol, Cyprus and Mytilene, Greece, deployed by Themistocleous et al. (2020), and Topouzelis et al. (2019) respectively. Remote sensing data from the two locations was downloaded and corrected using the ACOLITE atmospheric correction processor. In order to develop the classification models, 6 out of 12 Sentinel-2 bands were selected, which were blue (Band 2), green (Band 3), red (Band 4), red edge 2 (RE2) (Band 6), near infrared (NIR) (Band 8), and short-wave infrared 1 (SWIR1) (Band 11), as well as two indices NDVI and FDI. The use of NDVI and FDI has been proven to be effective in detecting floating plastics as discussed previously in an experiment conducted by Biermann et al. 2020 thus they were selected to develop the models.

Basu et al. (2021), had no prior knowledge about the classification algorithm that would produce the highest accuracy in detection of floating marine plastic, thus, two unsupervised (K-means and Fuzzy C-means (FCM)) and two supervised (Support Vector Regression (SVR) and Semi-supervised Fuzzy C-means (SFCM)) classification algorithms were considered. Unsupervised classification is a tool used to classify pixels in remote sensing images that does not require training data. This means that the algorithm will group pixels together according to their spectral properties, the user can alter the number of classes the algorithm will generate, and must assign the name of the classes manually, such as "Plastic", "Clean Deep Water", "Shallow Water" etc. Unlike unsupervised classification algorithm, supervised classification requires the user to select "training sites", which are pixels containing spectral properties of the desired classes. The spectral signatures of the training pixels will then be recognized and further applied to the entire image, classifying each pixel into a defined class based on your training data. For this reason, it was important to have in-situ data, not only to verify the accuracy of the algorithms, but also to have clear information on presence or absence of plastic that could be used as training data (GISGeography, 2022).

The unsupervised classification algorithms (K-means and Fuzzy C-means) relied only on the remote sensing imagery and did not use any in-situ data. The supervised classification algorithms (Support Vector Regression and Semi-supervised Fuzzy C-means) required in-situ data as an input for the training data, which was used to calibrate the classification model. Once the model was calibrated, it was validated using the in-situ data and could be applied in other locations where the presence of floating plastic was unknown. From a previous study conducted by Biermann et al. 2020 it was evident that the Floating Debris Index and the Normalized Difference Vegetation Index are useful in detection of floating marine plastic, as well as the red, NIR, RE2 and SWIR1 bands. However, it was not known prior which combination of bands and indices would produce the optimal result in plastic detection. Basu et al. 2021, composed an attribute set of three

categories that contain different combinations of bands and indices, and fed them into the supervised and unsupervised classification algorithms (Figure 3.5).

Attribute Set	Bands/Indices Used
A	(i) Blue, (ii) Green, (iii) Red, (iv) RE2, (v) NIR, and (vi) SWIR1, and two indices (vii) FDI, and (viii) NDVI
B	(i) Red, (ii) RE2, (iii) NIR, and (iv) SWIR1, and two indices (v) FDI, and (vi) NDVI
C	(i) FDI and (ii) NDVI

Figure 3.5: *Table depicting attribute sets used to compare classification algorithms combosed by Basu et al. (2021)*

The total available training data was divided into the calibration and validation sets, in order to ensure that the validation data was not used as an input into the model. The four classification algorithms were tested and compared using the error/confusion matrix, the F-score, and the overall accuracy. The highest accuracy was found when using the SVR supervised classification algorithm when attribute set "A" was used as an input, which included all 6 bands as well as the FDI and NDVI indices, with an overall accuracy of 98.4%. For all four classification algorithms, using attribute set "A" showed the highest overall accuracy results. The SVR, the FCM algorithm showed second highest accuracies in all three attribute sets, with attribute set "A" being the highest. Figure 3.6 depicts the four classification algorithms as well as their accuracies when used with attribute sets "A", "B", and "C".

Algorithm	Attribute	A				B				C			
	Modelled	Observed		OA (%)	F-Score	Observed		OA (%)	F-Score	Observed		OA (%)	F-Score
		Plastic	No Plastic			Plastic	No Plastic			Plastic	No Plastic		
K-means	Plastic	12	21	81.4	0.50	12	25	78.3	0.46	12	36	69.8	0.38
	No Plastic	3	93			3	89			3	78		
FCM	Plastic	13	21	82.2	0.53	12	21	81.4	0.50	12	36	69.8	0.38
	No Plastic	2	93			3	93			3	78		
SVR	Plastic	13	0	98.4	0.93	12	0	97.7	0.89	11	0	96.9	0.85
	No Plastic	2	114			3	114			4	114		
SFCM	Plastic	14	45	64.3	0.38	14	45	64.3	0.38	2	21	35.7	0.05
	No Plastic	1	69			1	69			13	44		

Figure 3.6 *Performance matrix of the four classification algorithms, K-means, Fuzzy c-means, Support vector regression, Semi-supervised fuzzy c-means when using Attribute Sets, A, B, and C. OA being the overall accuracy, and the numbers in the confusion matrix being the number of grids belonging to the validation set. Composed by Basu et al. (2021).*

Basu et al. (2021), stated that using the FDI and NDVI indices along with the six bands (blue, green, red, NIR, RE2, and SWIR) shows a higher performance in identifying floating plastic, than when the indices or bands were used alone. The study clearly demonstrated the ability of machine learning algorithms to identify floating marine plastics using freely available remote sensing data. It is important to mention that this study used Sentinel-2 imagery with a maximum resolution of 10 meters. The plastic

targets serving as in-situ information for this experiment were either 10 x 10 meters or larger. Basu et al. 2021 noted that floating plastics in real marine environments are not always covering the entire grid of the remote sensing data. This presents a challenge due to most open access satellite data having the highest spatial resolution of 10 meters, meaning smaller patches of marine plastic debris will simply not be recognized by the satellite.

Another study conducted by Freitas et al. (2021), explored the use of hyperspectral imaging system for detecting plastic debris in the ocean. Unlike previously discussed studies, instead of the optical sensor of the Sentinel-2 satellite, the study aimed to compare the use of a hyperspectral sensor aboard manned and unmanned aircrafts. The MSI sensor of Sentinel-2 Satellite has only 13 bands, meanwhile the hyperspectral sensors can contain hundreds of narrow bands covering almost the entire electromagnetic spectrum. This means that hyperspectral sensors are more sensitive to the spectral properties of different objects on Earth and could potentially be very effective in distinguishing marine debris from other materials (Wasser, 2023). The study also explored automated detection of marine plastic by testing two supervised classification algorithms. The two classification algorithms were Random Forest (RF) and Support Vector Machines (SVM).

Freitas et al. (2021) first characterized the spectral characteristics of marine plastic samples under different conditions such as amount of sunlight, time of day, as well as wet and dry samples. This spectral response was recorded by a hyperspectral camera (Specim FX10e), in a laboratory, which was placed 1 meter above the marine litter samples. The two other means of analyzing plastic's spectral properties using a hyperspectral sensor included a manned aircraft (A Cessna F150L) and an unmanned aerial vehicle (Grifo-X). The two aircrafts observed plastic targets in Faial Island Azores from 16th to 25th of September of 2020. Similarly to the experiment conducted by Topouzelis et al. (2019), the targets had a 10 x 10 meter resolution to match the resolution of the Sentinel-2 satellite. A 10 by 10 meter object on the Earth's surface will be equivalent to 1 by 1 pixel of the Sentinel-2 satellite. The two aircrafts were launched to fly above the plastic targets at different altitudes, a few moments before or after Sentinel-2 satellite would fly over

the area. Freitas et al. (2021) noted that the data collected by the multispectral sensor of the Sentinel-2 satellite was contained less reliable information than the aircrafts' data, due to the effects of cloud cover. Sentinel-2's multispectral data is affected by cloud cover since clouds block direct sunlight from hitting the objects. This leads to variations in the energy of the reflections as well as the absorption coming from the objects on Earth's surface (Arroyo-Mora et al. 2021).

Results of the hyperspectral signatures of plastic retrieved from the laboratory as well as from the two aircrafts were similar, proving that altitude of the UAV does not affect spectral responses. Multispectral data from Sentinel-2 however, could not be compared due to the effect of cloud cover interfering with the signal. Furthermore, the two classification algorithms Random Forest and Support Vector Machines were trained with the data from the 18th September, 2020, flight of the manned aircraft. The two algorithms were then tested using data collected over the same area on the 20th September of 2020. Their results showed that SVM has a higher accuracy than the RF algorithm in detecting plastic targets overall, however RF algorithm provided more consistent results when it did detect a target. The study concludes that the RF and SVM classification algorithms have the potential to detect plastic marine litter with a 0.70 – 0.80 precision when using a hyperspectral sensor at a 600-meter altitude. Freitas et al. (2021) noted that developing unsupervised classification algorithms could aid in the process of automated detection of marine litter. The study also stated that looking into spectral unmixing techniques could expand the quality and quantity of marine plastic detection.

Previously mentioned studies focused mainly on the detection of floating plastics by using known in-situ data on the presence of plastic. The in-situ data came in a form of plastic targets, first set up during the Plastic Litter Project: 2018 by Topouzelis et.al (2019), and their team at the University of Aegean. As discussed in the earlier paragraphs of this section, the targets that were deployed had a 10 x 10 meter area, which is Sentinel-2's highest resolution. Topouzelis et al. (2020) decided to continue this study on plastic litter monitoring from space, however the objective was to use 5 x 5 m and 1 x 5 m targets which are below the highest resolution of Sentinel-2 satellite. This study, known as the Plastic Litter Project: 2019 (PLP2019), would resemble more realistic conditions on the

presence of floating plastic in the ocean. The structure of targets created for the PLP2019 composed of pipes made from polyvinyl chloride (PVC), which is a common plastic polymer. The targets themselves were composed individually of polyethylene terephthalate (PET) (plastic bottles), polyethylene (plastic bags), and natural debris (reeds). The PLP2019 was conducted in the same location as PLP2018, Mytilene, Greece, where the targets were set up every five days off the coast of the beach to match Sentinel-2's flight path. The targets were first set up on April 18, 2019, up until June 7 of 2019.

In total 5 Level-1C and Level-2 cloud free images were acquired from the Sentinel-2 Satellite using Copernicus Open Access Hub. The study used the ACOLITE atmospheric correction processor to perform atmospheric corrections on the Level-1C images and remove the sun glint. Exact position of plastic targets was recorded by an UAV which captured the target's exact position on the same day that the Sentinel-2 satellite would fly overhead. The percentage of plastic in each Sentinel-2 pixel was calculated by an object-based image analysis. This process included isolating the pixels at the testing site and extracting the percentage of plastic pixel coverage based on the UAV images. Furthermore, the study extracted spectral data from each plastic target. This study used the inverse spectral unmixing technique to derive spectral signatures of the plastic targets. Since the percentages of plastic was already calculated in the previous step, it was possible to use this variable as an input to the inverse spectral unmixing formula, which, as a result, will provide an estimation of the spectral response of the plastic targets. Furthermore, this study utilized the use of matched filtering which is another technique to calculate the occurrence of a known material in a pixel by increasing the response from the known material and suppressing the signals from the background (Topouzelis et al. 2020).

The study generated a spectral curve graph of the plastic targets (Figure 3.7) and found that plastics have a peak in the NIR and a high reflectance in the visible range. This finding is correlated with the spectral graph created by Biermann et al. (2020), which was mentioned earlier in this section. The study also noted that when a plastic target consisting of plastic bags was wet, or even submerged by water, the spectral response was very weak and the plastic could not be distinguished from the surrounding water.

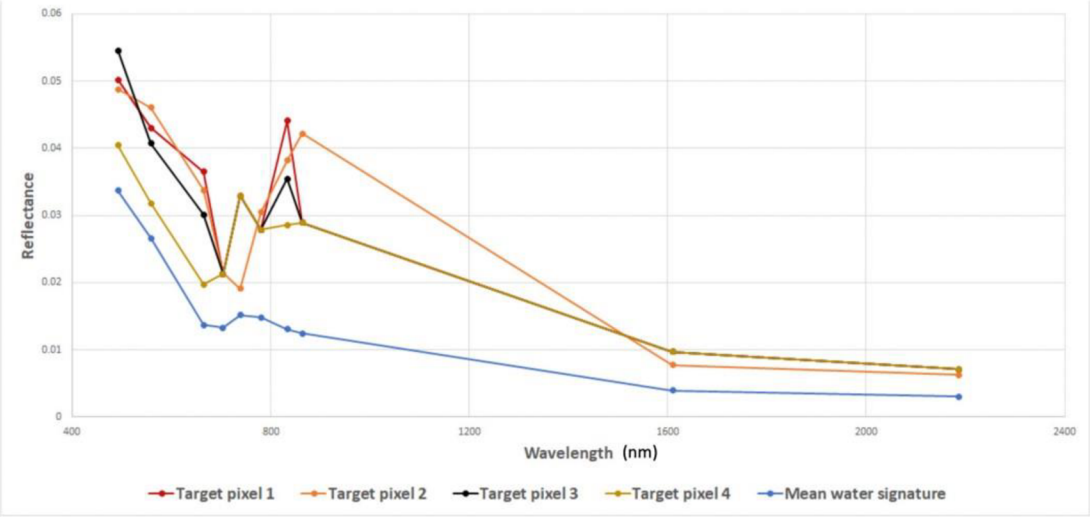

***Figure 3.7**: Spectral signature graph generated by Topouzelis et.al (2020) for the Plastic Litter Project 2019, with each target pixel containing a different percentage of floating plastic in relation to the total pixel area. https://www.mdpi.com/2072-4292/12/12/2013*

The matched filtering technique was applied to all six images of the PLP19 acquired from April 2018 to June 2019. The study concluded that the matched filtering approach was successful at detecting floating marine plastic with the use of a known spectral signature, in this case the signature of PET. In other words, pixels that contain a bigger percentage of debris, were identified as having a bigger percentage of debris by this method. Furthermore, the matched filtering process was successful when using the PET spectral signature, when the fractional abundance of PET was at least 25%. This means that the algorithm would detect the presence of a 25 square meters plastic patch in a 100 square meters pixel.

Author/Authors	Name of Study	Location of Study Area	Satellite, Sensor	Method	Year
Basu et al.	Development of Novel Classification Algorithms for Detection of Floating Plastic Debris in Coastal Waterbodies Using Multispectral	Limassol, Cyrus, Mytilene Greece	Sentinel-2, MSI	Supervised/Unsupervised Classification algorithms	2021

	Sentinel-2 Remote Sensing Imagery				
Biermann et al.	Finding plastic patches in coastal waters using optical satellite data	Scotland, Ghana, South Africa, Vietnam, Canada, Greece	Sentinel-2, MSI	Spectral data acquisition + Indices	2020
Freitas et al.	Remote Hyperspectral Imaging Acquisition and Characterization for Marine Litter Detection	Faial Island, Portugal	Hyperspectral sensor aboard UAV	Hyperspectral signature analysis + classification algorithms	2021
Topouzelis et al.	Detection of floating plastics from satellite and unmanned aerial systems (Plastic Litter Project 2018)	Mytilene, Greece	Sentinel-2,MSI, UAV, Sentinel-1, SAR	Spectral signal analysis	2018
Topouzelis et al.	Plastic Litter Project 2019: Exploring the Detection of Floating Plastic Litter Using Drones and Sentinel 2 Satellite Images	Mytilene, Greece	Sentinel-2, MSI ,UAV	Spectral signature analysis + Spectral unmixing	2019

***Table 1**: Summary of literature review examined in this study including the authors, name of study, location of study area, satellite/sensor used, method, and year that study was conducted. With MSI standing for Multispectral Instrument and UAV standing for Unmanned Aerial Vehicle.*

4. Characteristics of study area and in-situ data

To perform further analysis of floating plastic debris, this study used in-situ data of floating plastic targets from previously conducted experiments to propose an alternative algorithm for floating plastic detection. The two main locations of plastic targets were in Mytilene, Greece, and Limassol, Cyprus, and the images were obtained from the Copernicus Open Access Hub database. Topouzelis et al. (2019), conducted the Plastic Litter Project 2018 (PLP18), where on June 06 and 07, 2018 three plastic targets were set up about 30 meters away from the coastline of Tsamakia Beach of Mytilene, Greece. The

three targets being 10 x 10 meters in size, consisted individually of plastic bottles, plastic bags, and plastic fishing nets. The targets were placed on those dates keeping in mind that the Sentinel 1 and 2 satellites would be flying above the area. A similar experiment was again conducted by Topouzelis et al. (2020), where on April 18, 2019, 45 x 5 meter plastic targets were deployed in the same location of Mytilene, Greece with the targets consisting of 50% plastic bottles and 50% plastic bags. The same year on May 3 (2019) Topouzelis et al. placed 45 x 5 meter targets, as well as 21 x 10 meter targets some consisting of plastic bottles, while others consisting of plastic mesh and plastic bags. On June 07, 2019 more plastic targets 45 x 5 meters in size were placed in the same location by Topouzelis' team. On December 15, 2018 Themistocleous et al. (2020) placed a 3 x 10 meter target, 200 meters from the coastline of Old Port in Limassol, Cyprus. The target was made up of solely plastic bottles, tied together with a nylon string. The date of the experiment was selected according to the Sentinel 2 satellite overpass.

***Table 2**: Description of the satellite images downloaded for this study, including date of acquisition, satellite type, full path of satellite image, and the location where the plastic targets were set up.*

IN SITU DATA ON THE PRESENCE OF PLASTIC

Date Of Acquisition mm/dd/yyyy	Satellite	Path	Location
06/07/ 2018	2A	S2A_MSIL1C_20180607T085601_N0206_R007_T35SMD_20180607T110513	Mytilene, Greece
12/15/ 2018	2A	S2A_MSIL1C_20181215T083341_N0207_R021_T36SWD_20181215T085809	Limassol, Cyprus
04/18/ 2019	2B	S2B_MSIL1C_20190418T085559_N0207_R007_T35SMD_20190418T110441	Mytilene, Greece
05/03/ 2019	2A	S2A_MSIL1C_20190503T085601_N0207_R007_T35SMD_20190503T103221	Mytilene, Greece
06/07/ 2019	2B	S2B_MSIL1C_20190607T085609_N0207_R007_T35SMD_20190607T110335	Mytilene, Greece

Figure 4.1: *Areas of interest containing in situ data of the presence of plastic, (top) Mytilene, Greece, (bottom) Limassol, Cyprus*

5. Methodology

5.1 Sentinel-2 data and atmospheric correction

In total 5, Sentinel-2 Level 1-C multispectral images were downloaded from Copernicus Open Access Hub Open Access Hub (copernicus.eu). Level 1-C data produces Top of the Atmosphere reflectance values meaning values that have not been adjusted prior by an atmospheric corrector. It is possible to download already atmospherically corrected (Level 2A) data for the same dates. The European Space Agency (ESA) running the Copernic Open Access Hub provides the so-called Bottom of the Atmosphere reflectance values (Level 2A) which have been atmospherically corrected meaning certain effects of the atmosphere such as cloud coverage was removed. Furthermore, the atmospherically corrected images can provide you with the information on different conditions at the time of the image collection such as water vapor or sun angle (ESA, 2023). In this study Level 1C data was downloaded with the purpose of performing independent atmospheric correction of images using the C2RCC (Case 2 Regional Coast Color) atmospheric correction processor. Typically, atmospheric correction processors are designed for land surface images, showing less accuracy when applied to water areas. For instance, ESA's Sen2Cor processor is based on the dark dense vegetation approach, where the algorithm considers vegetation as sufficiently dark, and requires certain pixels in the image to correspond to the dark dense vegetation (Pereira-Sandoval, 2019). This atmospheric corrector may not be optimal when considering images consisting mostly of water. The C2RCC is open source and can be accessed through the SNAP (ESA's Sentinel Application Platform) in the Sentinel Toolboxes. This atmospheric correction processor was developed with the aim to atmospherically correct as well as to retrieve certain components in the water (C2RCC.org, 2023). The output of C2RCC includes atmospherically corrected bands, various inherent optical properties, as well as concentrations of different substances in the water.

5.2 Using multispectral satellite imagery to obtain optimal plastic recognition

Pre-processing of satellite imagery

This study aims to use freely available multispectral remote sensing imagery to inspect various bands, band combinations, and indices to identify floating plastic in the

marine ecosystem. In Section 4 of this study the description and acquisition of the in-situ data can be found. It is important to perform pre-processing before analyzing spectral properties of the in-situ plastic targets. The pre-processing of remotely sensed images often includes two steps, the radiometric correction (image enhancement), and geometric correction (georeferencing). Pre-processing allows for the correction of some distortions and helps increase the overall quality of the images for a more accurate image analysis. More specifically performing radiometric correction helps calibrate the effects of the atmospheric condition, the sun's illumination, and other outside factors present during image acquisition. The process of geometric correction allows for the reduction of spatial errors by adjusting the remotely sensed image to a desirable coordinate system (Wageningen University, GIMA). This study used ESA's SNAP remote sensing software to perform all processing and analysis of the remote sensing data. All Sentinel-2 Level 1C data used in this study underwent geometric correction, more specifically the S2 Resampling Processor was used for all the images. Resampling is a technique that allows for the manipulation of resolution, along with other applications such as change of orientation or change of rotation of the image (Gurjar, 2005). The images in this study were resampled to have an output resolution of 10 meters for all bands. The upsampling method used was "Bilinear", while the down sampling method used was "Mean". Resampling is also required for the files to be an input into the C2RCC atmospheric correction processor mentioned previously. Subsets of the resampled images were then created in order to reduce the amount of data and minimize processing time for the next steps. All Sentinel-2 images were processed with the C2RCC atmospheric correction processor. As mentioned previously in Section 4.1, the output of the C2RCC atmospheric correction processor includes various inherent optical properties which are useful for the analysis of water characteristics. Moreover, the outputs include the scattering and absorption of various components, such as the absorption of phytoplankton pigments, or the scattering coefficient of marine particles. The outputs of the C2RCC were relevant for the creation of appropriate plastic detection formula.

Selection of appropriate plastic and sea pixels, and satellite derived variables

In order to evaluate the optimal bands, combination of bands, or indices needed for plastic recognition. Reflectance values of in-situ data were gathered, along with reflectance information of pixels at different water depths in each image. This process required pins to be placed at each pixel where plastic targets were present. Information regarding the location of the plastic targets for Limassol, Cyprus is described in detail by Themistocleous et. al (2020), meanwhile data for Mytilene, Greece is available at: PLP2019 dataset | Zenodo. The pins were placed on the location of each pixel containing a plastic target in a particular image, furthermore three pins each were placed randomly for pixels at shallow, medium, and deep water levels in each image. In total 59 pins were placed on plastic targets, meanwhile 45 pins were placed on water pixels. The pixels values from the atmospherically corrected Bands 2 (Blue), 3 (Green), 4 (Red), and 8 (NIR), as well as the inherent optical properties (iop_adet, iop_agelb, iop_apig, iop_atot, iop_bpart, iop_bwit), were extracted into a table. Furthermore, the Plastic Index (PI) was applied on each of the images and its values for each pixel were extracted. The Plastic Index was generated and tested in a study by Themistocleous et. al (2020) where it was tested on plastic targets of various sizes deployed in Limassol, Cyprus. The PI utilizes bands 4 (Red) and 8 (Near Infrared) of the Sentinel-2 satellite in the following formula: *PI = B08/(B08 + B04)*. Their study tested various indices; however, the PI had shown to be the most optimal in identifying the plastic targets, thus it was chosen as a variable in this study. The following table provides detailed information about the values extracted from different bands and indices for each pixel.

***Table 3**: Description of the bands and indices from which pixel values were extracted in each satellite image.*

Chosen Bands and Indices for the Extraction of Values

Bands	**Color**	**Central Wavelength**
Band 2	Blue	490nm
Band 3	Green	560nm
Band 4	Red	665nm
Band 8	Near Infrared	842nm
IOP	**Description**	

iop_adet	Absorption coefficient of detritus
iop_agelb	Absorption coefficient of gelbstoff
iop_apig	Absorption coefficient of phytoplankton pigments
iop_atot	Phytoplankton + detritus + gelbstoff absorption
iop_bpart	Scattering coefficient of marine particles
iop_bwit	Scattering coefficient of white particles
Index	**Formula**
Plastic Index (PI)	(Band 8)/(Band 8 + Band 4)

*Complete table of extracted values used for the analysis can be found in the Appendices section of this study (Table 11.1).

Testing algorithms for optimal plastic detection using R studio

To visualize the distribution of values in each band and index, the data values were uploaded into the R studio software which is designed for statistical computation and creating graphics for large sets of data. Boxplots were generated for each individual image as well as for all images combined. Boxplots for individual dates can be found in the Appendices section of this study.

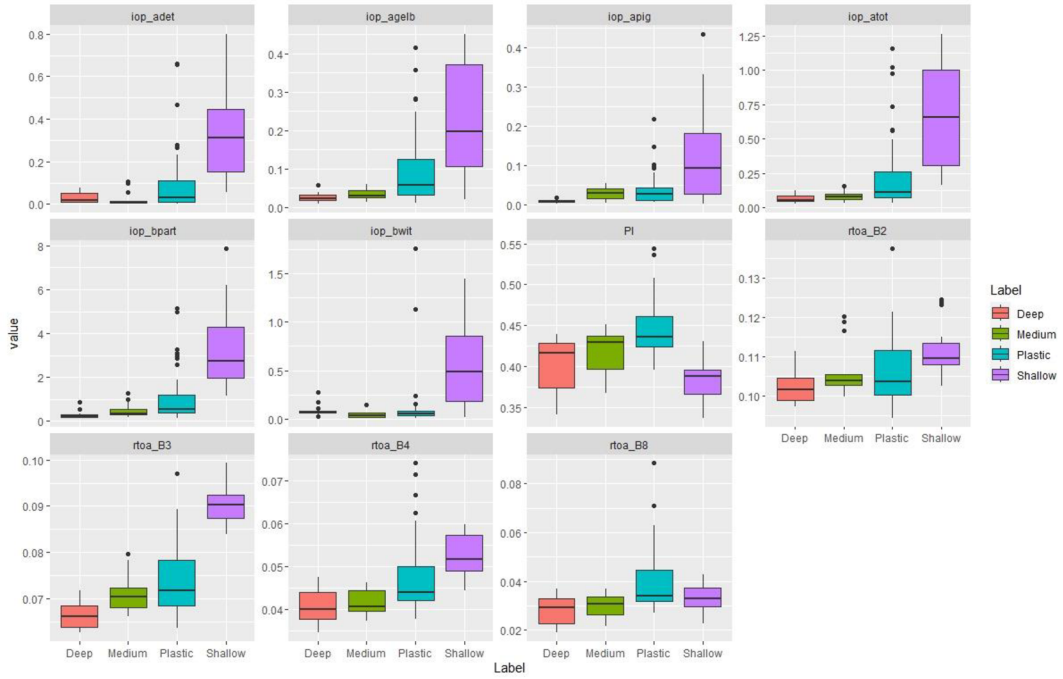

Figure 5.1 *Boxplots depicting the overall distribution of values among individual bands and indexes for all images from December 15, 2018 to June 07, 2019. Rtoa_B2, rtoa_B3, rtoa_B4, rtoa_B8, being Bands 2, 3, 4, and 8 respectively.*

To predict the presence or absence of plastic in pixels, the extracted data from the selected bands and indices was tested with the Random Forest algorithm. The Random Forest algorithm, (also known as Breiman and Cutler's Random Forests for Classification and Regression) can be accessed through a package 'randomForest' in the R Studio software. Detailed description of the algorithm related to usage, arguments, and examples can be accessed with the following link: randomForest: Breiman and Cutler's Random Forests for Classification and Regression (r-project.org) . The Random Forest algorithm works similarly to the Decision Tree algorithm; however, it produces a model with a lower variance, meaning the results are not overfit. The Random Forest algorithm uses a technique known as Bootstrap Aggregation created by Leo Breiman. In this technique samples from the original dataset are randomly selected and placed in a new dataset of a smaller size, making these samples independent from each other. These datasets are then inputted in the model and all the results from the model are combined into one final output (Bento, 2021). The exact code for the Random Forest algorithm, as well as the visualization of the distribution of pixel values used in this study can be found in the Appendices - Section 11, Figure 11.7.

5.3 Using a spectroradiometer to measure the reflectance of different plastic samples occurring in marine debris

According to GESAMP (2019), plastics are defined as synthetic polymers that have thermo-set characteristics, meaning they are made from hydrocarbon or other biomass raw materials. GESAMP(2019) characterize most plastics into two main categories: thermoplastics and thermoset. Thermoplastics such as polyethylene, polypropylene, and polystyrene, are plastics that have the capability to be broken down by heat. On the other hand, thermoset plastics such as polyurethane, paints, and epoxy resins do not break down under the influence of heat. They further explain that marine plastic litter is often mixed with other additives like colorants, stabilizers, and plasticizers. GESAMP (2019) created a table (Table 4) depicting the most common polymers found in marine debris as well as their common applications, specific gravity, and their behavior (ability to float or sink in the aquatic environment).

Polymer	Common applications	Specific gravity	Behaviour
Polystyrene (expanded)	Cool boxes, floats, cups	0.02-0.64	Float
Polypropylene	Rope, bottle caps, gear, strapping	0.90–0.92	
Polyethylene	Plastic bags, storage containers,	0.91–0.95	
Styrene-butadiene (SBR)	Car tyres	0.94	
Average seawater		***1.03***	
Polystyrene	Utensils, containers	1.04–1.09	Sink
Polyamide or Nylon	Fishing nets, rope	1.13–1.15	
Polyacrylonitrile (acrylic)	Textiles	1.18	
Polyvinyl chloride	Thin films, drainage pipes, containers	1.16–1.30	
Polymethylacrylate	Windows (acrylic glass)	1.17-1.20	
Polyurethane	Rigid and flexible foams for insulation and furnishings	1.20	
Cellulose Acetate	Cigarette filters	1.22–1.24	
Poly(ethylene terephthalate) (PET)	Bottles, strapping	1.34–1.39	
Polyester resin + glass fibre	Textiles, boats	>1.35	
Rayon	Textiles, sanitary products	1.50	
Polytetrafluoroethylene (PTFE)	Teflon, insulating plastics	2.2	

***Table 4**: Common polymers found in the marine environment along with their applications, specific gravity, and behavior (ability to float or sink in the marine environment), GESAMP 2019 modified from GESAMP 2016.*

In this study, the spectral reflectance of various materials was measured using a spectroradiometer. A spectroradiometer is a device that is able to analyze electromagnetic wavelengths of various materials by having a built-in radiation source as well as analysis equipment. Main types of spectroradiometers include emission, absorption, and Fourier-transform type of device. In an emission spectroradiometer the built-in radiation source is able to capture electromagnetic wavelengths of various materials by shining a bright light directly at the material, and measuring the radiation emitted from them. The absorption spectroradiometer is able to detect various wavelengths by passing a known wavelength directly through a sample, while the detector system measures the absorption of the wavelength. Lastly the Fourier-transform spectroradiometer works similarly to the absorption spectroradiometer, except using a radiation of a broad band and producing an absorption spectrum of a material (Encyclopædia Britannica, 2018).

In this analysis the Malvern Panalytical ASD Leaf Clip was used to aid in measuring reflectance data of nine different plastic samples. The Leaf Clip accessory is commonly used in field measurements, specifically on live vegetation, as its structure allows vegetation samples to be placed inside and analyzed without inflicting damage. In

this case the Leaf Clip was used to accommodate the various shapes and sizes of selected plastic samples. The Leaf Clip has a lock/release system where an object of interest is placed and its' spectral properties are then analyzed by a spectroradiometer. The Leaf Clip is equipped with a head that contains a rotating panel with black and white faces, the white panel is used for transflectance while the black for reflectance (Malvern Panalytical, 2019). In this experiment the white panel with no samples inside was used first, to calibrate the spectroradiometer. After the spectroradiometer was calibrated, the target was changed to the black panel, which produced a spectral reflectance of zero. Based on previous literature review from GSAMP 2019, nine types of plastic samples commonly found in marine debris were collected and analyzed using the spectroradiometer. The nine samples were adjusted in size to fit inside the ASD Leaf Clip. Each sample of plastic was measured individually and its spectral curve was recorded to a text file, after which a spectral graph was generated using Microsoft Excel. The following table (Table 5) shows ten measurements that were taken and analyzed with the spectroradiometer:

Materials Used in Spectroradiometer Analysis

Black Panel Target	-
Type of Plastic	**Common Uses**
Poly(ethylene terephthalate) (PET)	Plastic Bottle
Cellulose Acetate	Cigarette Filter
Polystyrene	Container
Closed-cell extruded polystyrene foam	Styrofoam
Polyethylene	Bubble Wrap
Polyethylene	Layered Bubble Wrap
Polyethylene	Plastic Bag
Styrene-butadiene (SBR)	Rubber
Polystyrene	Utensils

***Table 5**: Materials collected and tested for spectral curve generation of plastic debris, including the type of plastic category they belong to and some of their most common uses.*

6. Current state of play

Although many new methods and algorithms are being developed for floating plastic detection, there are a few important aspects that must be considered that could present issues and challenges. In this study, the in-situ data collected for the verification of the plastic detection algorithms was acquired from experiments of Topouzelis et. al (2019, 2020), and Themistocleous et. al (2020). These studies performed experiments where they placed artificial plastic targets, made from various plastic materials, in the water on days that the Sentinel-2 satellite would fly over the area. The in-situ data from these experiments is crucial for many similar studies and can be accessed freely through the Copernicus Open Access Hub. However, due to the fact that such studies are not common, the in-situ data of plastic is limited. Due to the atmospheric condition, some images that were downloaded contained a substantial amount of cloud coverage, which made them unusable for plastic detection. This study was able to use five images containing a total of 59 pixels where plastic was present. Having a bigger in-situ dataset could alter the results of the algorithm, thus must be considered when judging its effectivity. Furthermore, choosing an appropriate atmospheric corrector is crucial in optimal plastic detection, as it plays a role in the response of the plastic spectral signal. Performing more measurements using the spectroradiometer can be very useful to determine whether the atmospheric corrector is returning accurate spectral signatures. A total of nine samples were collected for the measurement of a spectral signal of various commonly found debris using a spectroradiometer. Acquiring a wider range of samples could also provide a more defined spectral curve when averaging all the curves from the materials.

Additionally, the placement of pins to extract properties of shallow, medium, and deep water was purely random, in situ measurements of water depth were not taken in the area as this study is not focused on the water aspect. However, the results of the algorithms used will contain information on the classification of water pixels as well. It is important to note that the sensitivity of the classification algorithm for water depths should not be taken into account when evaluating the accuracy of the algorithm, as it has been trained focusing on the detection of plastic.

7. Results

7.1 Spectral graph of plastic samples

The Leaf Clip spectroradiometer was used in this study to measure the spectral properties of nine plastic samples commonly found in marine debris. The type of plastic samples used in this part of the study was based on literature from GESAMP (2019), where most common occurring polymers in floating plastic debris were identified. Detailed information on the type of plastic polymer as well as the samples used, can be found in Table 5 of Section 5.3 of this study. The generation of the spectral graph of the samples aids in understanding of the spectral behavior of plastic, and can help in identifying the correct method for floating plastic detection. Figure 7.1 shows the trends and patterns of plastic's reflectance along the electromagnetic spectrum. The "Black Target" sample was an additional measurement used to see the results of the calibration of the spectroradiometer, therefore, its spectral reflectance is close to zero. Five out of the nine samples produced a distinct spectral curve (polyethylene (plastic bag), cellulose acetate (cigarette filter), polystyrene foam (styrofoam), polyethylene (layered bubble wrap), and styrene-butadiene (rubber). The other four samples, (polyethylene (bubble wrap), polystyrene (container), poly(ethylene terephthalate) (plastic bottle), and polystyrene (utensils), did not produce a distinct spectral curve, having a reflectance below zero. Detailed information about the patterns and trends of the spectral curves is discussed in Section 8.1 of this study.

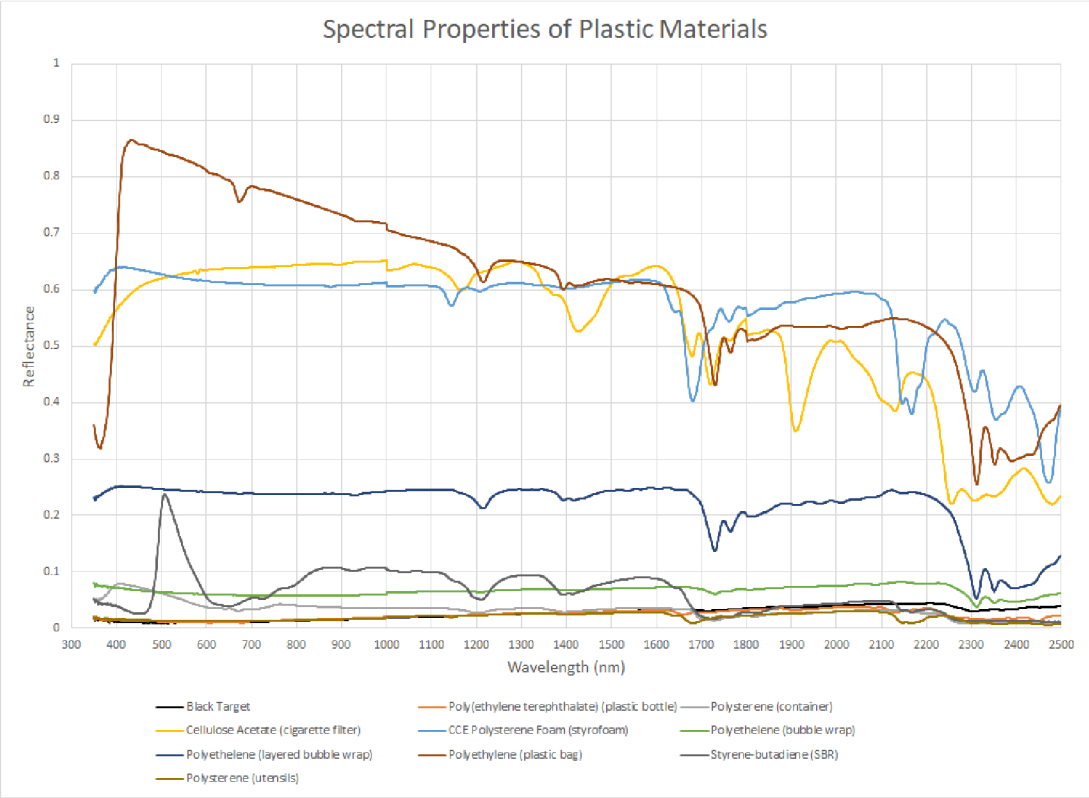

***Figure 7.1**: Spectral reflectance of commonly found plastics in marine debris generated with a spectroradiometer.*

7.2 Algorithm for optimal plastic detection

As mentioned previously in the Methodology Section 5.2, the Random Forest algorithm was chosen to test the optimal detection of plastic. Five Sentinel-2 images (Table 2) that contained in-situ data about the presence of plastic were downloaded and processed. Pixel values were extracted from each of the images containing information about plastic, as well as shallow, medium, and deep water. Pixel values from bands 2 (blue), 3 (green), 4 (red), 8 (near-infrared), as well as inherent optical properties iop_adet, iop_agelb, iop_apig, iop_atot, iop_bpart, iop_bwit, and the plastic index (PI) were chosen as variables in the Random Forest algorithm. Detailed description of the chosen variables can be found in Table 3 of Section 5.2 of this study. The variables considered for this study were picked based on their distribution in the boxplot (Figure 5.1), the bands/indices where the plastic distribution differed from the other three classes (shallow,

medium, deep water) were considered to be superior, and were chosen as in input to the Random Forest algorithm. Different combinations of the bands and indices were fed into the algorithm to see which of the combinations would produce the highest sensitivity to plastic. Four classes were used in the algorithm which were plastic, as well as, deep, medium, and shallow water. The best results were produced when the combination of PI, iop_adet, iop_agelb, iop_bpart, band 2, band 3, band 4, and band 8 was used. Using these variables, the algorithm detected 54 out of 59 pixels of plastic with the overall sensitivity to plastic being 91.5%. The following table presents the Confusion Matrix depicting the predictions of the Random Forest Classification algorithm:

Table 6: *Confusion matrix produced by the Random Forest Classification Algorithm using the combination of PI, iop_adet, iop_agelb, iop_bpart, band 2, band 3, band 4, and band 8 of the Sentinel-2 satellite.*

Random Forest Classification Correct vs. Predicted Values

Class	Deep	Medium	Shallow	**Plastic**
Deep	8	1	0	2
Medium	2	7	0	2
Shallow	0	0	13	1
Plastic	5	7	1	54

The overall accuracy for the classification of all classes was 78.9% with the Plastic class having the highest sensitivity of 91.5%. The sensitivity for classes Deep, Medium, and Shallow was: 53.3%, 46.7%, and 86.7% respectively. As mentioned previously, the model was not trained with the intention of recognizing various water depth classes, thus the algorithm was less sensitive to the three water classes than to the plastic class.

The following table (Table 7) presents the overall statistics by class based on the Random Forest algorithm when the optimal combination of PI, iop_adet, iop_agelb, iop_bpart, band 2, band 3, band 4, and band 8 was used:

Overall Statistics by Class				
	Deep	**Medium**	**Shallow**	**Plastic**
Sensitivity	0.533	0.467	0.867	0.915
Specificity	0.966	0.955	0.989	0.689
Prevalence	0.144	0.144	0.144	0.567
Detection rate	0.077	0.067	0.125	0.519
Balanced Accuracy	0.750	0.711	0.928	0.802

***Table 7**: Overall statistics of classes: plastic, deep, medium, and shallow water. Sensitivity: the percentage of "true positives" the model was able to distinguish. Specificity: the percentage if "true negatives" the model was able to distinguish. Prevalence: the occurrence of positive events, in relation to all positive and negative events. Detection Rate: percentage of true positives divided by the remaining true positive and false negative events. Balanced Accuracy: mean of sensitivity and specificity.*

8. Discussion

8.1 Spectroradiometer analysis: tends, pattens, and limitations

The collection, measurement, and analysis of nine different plastic samples commonly found in marine debris, allowed for the generation of a spectral reflectance graph. Due to the fact that plastics are composed from various polymer types, their spectral signatures are unique, yet still follow similar patterns along the electromagnetic spectrum. A few trends can be noticed where plastic samples tend to have a similar behavior. The first trend is a dip that occurs from 1100 – 1300 nanometers in six of the nine samples. These samples consist of polystyrene (utensils), cellulose acetate (cigarette filters), CCE polystyrene foam (styrofoam), polyethylene (layered bubble wrap), styrene-butadiene (SBR) (rubber), and polystyrene (container). The range of 1100 – 1300 nanometers lies between bands 9 and 10 of the Sentinel-2 satellite, meaning these bands can potentially be helpful in identifying some of the floating plastic marine debris. It is interesting to note that the spectral reflectance of the same material 'polyethylene' behaves differently depending on its structure. When layered on top of each other polyethylene sample (layered bubble wrap) produces a distinct dip around 1200 nanometers, however the same material shows no dip when only a single layer is measured. Although plastics in the marine environment are commonly layered together,

identifying single layers of thin transparent plastic, such as bubble wrap presents a challenge when looking solely at the reflectance curve. Another trend can be observed around 1400 nanometers, which lies between bands 10 and 11 of the Sentinel-2 satellite, these bands are both short-wave infrared (SWIR). Four of the nine samples show a slight dip in their reflectance in this range. The most coherent trend can be observed around 1700 nanometers where eight of the nine samples have a reduced reflectance, this again falls in the SWIR bands range of the Sentinel-2 satellite. Previously mentioned experiment by Topouzelis et al (2019), showed how plastic targets consisting of plastic bags, bottles, and fishing nets all reflect (show a distinct peak) in the near infrared (NIR) part of the spectrum (842 nanometers). The spectral graph created in this study does not show a distinct peak in NIR. It is a possibility that the samples used to measure spectral reflectance in this study did not show a peak due to the samples being too thin, as well as being transparent in color such as the Poly(ethylene terephthalate) (PET) (plastic bottle), polyethylene (bubble wrap), and polystyrene (container). Biermann et al. (2020) noted that individual pieces of plastic existing in a marine environment are not likely to be detected by satellites unless aggregated together into a larger patch. This could support the discrepancy of no reflectance in the NIR spectrum of this study, due to samples being too thin in their structure.

8.2 Optimal plastic detection using multispectral satellite imagery: influence of algorithm and atmospheric correction

One of the main aims of this study was to use freely available satellite imagery to develop an algorithm for optimal floating plastic detection. This study used Sentinel-2 satellite imagery from two sites where in-situ information about floating plastic was known: Limassol, Cyprus, and Mytilene, Greece. In total 59 pixels containing values that represented floating plastic's reflectance were extracted, along with 45 pixels containing information on the reflectance of various water depths: shallow, medium, and deep. The Random Forest algorithm was trained according to the in-situ data collected in this study. Although the algorithm and chosen variables (bands: 2, 3, 4 ,8, iop_adet, iop_agelb, iop_bpart, and the plastic index) showed very promising results, it is important to keep in mind that having a bigger set of training data could alter the results of the algorithm.

Unfortunately, studies such as the ones done by Topouzelis et. al 2019, 2020, and Themistocleous et al. 2020, are not very common. These studies aimed at testing satellites' capabilities at detecting floating plastic from space, by manually setting up plastic targets of various sizes on the days that Sentinel-2 satellite would fly overhead. These plastic targets are extremely useful for being able to analyze floating plastic's properties, and seeing the extent to which satellites can capture them. Having more large-scale experiments similar to the previously mentioned ones, could be extremely helpful for future studies.

The Random Forest algorithm chosen for this study was able to predict the presence of plastic with a 91.5% sensitivity, however the classes of different water depths (shallow, medium, and deep) had a lower sensitivity. This was due to the fact that when choosing the variables as an input, this study focused mainly on the distribution of values of plastic rather than water. This resulted in the overall accuracy of the algorithm being brought down to 78.9%. The Random Forest algorithm showed promising results in detecting the true positive events of plastic (91.5%), however the rate of detection of true negative results was much lower (68.9%), therefore the balanced accuracy of the plastic class was brought down to 80.2%. The shallow water class had the overall highest balanced accuracy (92.8%) out of the four classes meaning the algorithm accurately detected the most "true positive" and "true negative" events in this class. It could be useful for future studies to train the algorithm for correctly classifying both the plastic pixels as well as the water pixels to achieve an overall higher accuracy. Furthermore, it is important to pick appropriate variables in order to achieve the best results using a classification algorithm, Figure 5.1 in the methodology section of this study shows the distribution of values in various bands an indices. This information was very crucial in determining which variables and their combinations would be useful to detect plastic apart from other pixels. For instance, the distribution of values in the PI is much more isolated in the plastic category than in the water categories. Seeing these distributions in various bands and indices helped this study determine that bands 2 (blue), 3 (green), 4 (red), and 8 (near infrared) are useful in distinguishing plastic apart from water. This is also supported by a study done by Topouzelis et al. (2020), where a spectral graph was

generated that showed that in the visible (bands: 2, 3, and 4) and near infrared (band: 8) parts of the electromagnetic spectrum, plastic's spectral curve differed from water.

Additionally, when working with satellite images, it is crucial to pick an appropriate atmospheric correction processor. As mentioned previously, the atmospheric correction processor helps deduct the effects of clouds and other influences that can interfere with the reflectance coming from the surface. This study explored the use of Case 2 Regional Coast Color (C2RCC) atmospheric correction processor, which along with atmospherically correcting the images, provided informative properties of water pixels. Using C2RCC this study was able to extract values from new bands that contained information about the inherent optical properties of water such as the absorption coefficient of detritus. These new bands generated by C2RCC were useful in training the random forest algorithm to detect pixels containing plastic. Previously done studies such as the Plastic Litter Project 2018, conducted by Topouzelis et.al 2019, show that other atmospheric correction processors such as "ACOLITE", have end-products that contain useful information for the detection of floating plastic debris. ACOLITE atmospheric correction processor was found to have a higher performance in the 490 – 681 nm (visible) range, for atmospherically correcting coastal waters, compared to other commonly used atmospheric correction processors (Vanhellemont et al. 2021). Therefore, choosing an appropriate atmospheric corrector can play a big role especially when analyzing satellite images consisting mostly of water.

8.3 Consensus of related literature

In Section 3 of this study, previous literature on the methods of detection of floating plastic debris was gathered and examined. The common consensus is that the near infrared band (Band 8) of the Sentinel-2 satellite is one of the essential bands for detection of floating plastic debris. Biermann et. al (2020), confirmed that plastic materials strongly reflect light in the near infrared part of the electromagnetic spectrum, whereas water absorbs light in this area. They further noted that the combination of Floating Debris Index (FDI) and Normalized Difference Vegetation Index (NDVI), had the best results for forming clusters for individual materials commonly found in marine debris, meaning these indices were effective in isolating plastic from other materials. This

same conclusion is seen in the study by Basu et al. (2021), where various classification algorithms were tested for optimal detection of plastic. They confirmed that when using the FDI and NDVI together with six bands of the Sentinel-2 satellite (Bands: blue, green, red, near infrared, red edge-2, short wave infrared), the accuracy of detection of floating plastic was at its peak, having an overall accuracy of 98.4%. The study done by Topouzelis et al. (2020), during the Plastic Litter project 2019, also confirmed the previous finding that plastic shows a peak in the NIR and can be distinguishable from water at the visible spectrum (Bands 2 (blue), 3 (green), and 4(red)) of the Sentinel-2 satellite. Furthermore, the Plastic Index (PI), developed by Themistocleous et. al (2020), which was proven to be the most effective index for detecting floating plastic in their study, utilizes bands 4 (red) and 8 (near infrared) of the Sentinel-2 satellite, further adding to the consensus of the two studies mentioned previously. All the studies reviewed in the related literature section of this study concluded that plastic targets can be detected from space with the Sentinel-2 satellite at a 10 meter resolution, meaning a patch of floating plastics is covering a 10 x 10 meter pixel. Topouzelis et. al (2020) further conclude that detection of floating plastic from the Sentinel-2 satellite is even possible on a subpixel scale when using a spectral unmixing approach. Their study found that floating plastic detection on a subpixel scale is possible using the known spectral signature of a plastic sample with the matched filtering technique, as long as the plastic covers at least 25% of the whole area.

9. Conclusion

This study explored the capabilities and limitations of using of remote sensing systems for the purposes of floating plastic detection. The literature review in this study compared methods from different authors to demonstrate that remote sensing systems can successfully detect plastic from space, even on sub-pixel scales. Different approaches such as classification algorithms, spectral curve generations, and applications of indices, showed the versatility of detecting and monitoring floating plastic debris. Indices such as the Plastic Index (PI), have been proven to be successful in identifying floating plastic targets of a 3 x 10 meter size (smaller than a Sentinel-2 pixel). Additionally, this study

explored the use of a spectroradiometer to generate a spectral curve of commonly found plastic materials in marine debris. Previously done studies analyzing plastic's spectral properties concluded that plastic reflects light much greater than water in the visible (400 – 700nm) and near infrared (800 - 2500nm) parts of the electromagnetic spectrum. This confirms that bands 2 (blue), 3 (green), 4 (red), 8 (near infrared) of the Sentinel-2 satellite can contribute to the distinction of plastic apart from water pixels. When appropriate in-situ data of floating plastic is available, vital information about plastic's spectral properties can be analyzed and applied to methods of plastic detection. Furthermore, this study explored the use of the Random Forest classification algorithm in detection of floating plastic debris. Pixel values from different bands of the Sentinel-2 satellite were extracted and used as variables in the algorithm. The Case 2 Regional Coast Color atmospheric correction processor played a vital role in generating inherent optical properties whose values were also used as an input into the Random Forest algorithm. Using bands 2 (blue), 3 (green), 4 (red), 8 (near infrared), as well as the plastic index (PI), and a combination of the inherent optical properties, the Random Forest algorithm detected 54 out of 59 plastic pixels, having a 91.5% sensitivity to plastic.

The availability of remote sensing images where presence of plastic was known, served as crucial information for performing the analysis and testing the algorithm for floating plastic detection in this study. Having more studies done where plastic targets are set up to simulate floating plastic debris, would greatly impact the possibilities for further plastic detection, monitoring, and analysis. It is essential for more experiments to be conducted such as the Plastic Litter Project 2018 and 2019 with a wider range of plastic target sizes, structures, and locations, to simulate floating plastic debris in various conditions. Furthermore, this study proposes further research to explore the use of different atmospheric correctors and their capabilities in influencing plastic detection. Future studies can utilize the algorithm tested in this study on other satellite systems such as Synthetic Aperture Radar (SAR) to perform plastic detection below the surface of the water.

10. Bibliography

Arroyo-Mora, P., Kalacska, M., Løke, T., Schläpfer, D., Coops, N., Lucanus, O., Leblanc, G., 2021: Assessing the impact of illumination on UAV pushbroom hyperspectral imagery collected under various cloud cover conditions, Remote Sensing of Environment, Volume 258, 112396, ISSN 0034-4257, (on-line): https://doi.org/10.1016/j.rse.2021.112396.

Basu, B., Sannigrahi, S., Basu, A. S. S., Pilla, F., 2021: Development of Novel Classification Algorithms for Detection of Floating Plastic Debris in Coastal Waterbodies Using Multispectral Sentinel-2 Remote Sensing Imagery, (on-line): (PDF) Development of Novel Classification Algorithms for Detection of Floating Plastic Debris in Coastal Waterbodies Using Multispectral Sentinel-2 Remote Sensing Imagery (researchgate.net) .

Bento, C., 2022: Random forests algorithm explained with a real-life example and some python code. Medium. (on-line): https://towardsdatascience.com/random-forests-algorithm-explained-with-a-real-life-example-and-some-python-code-affbfa5a942c

Biermann, L., Clewley, D., Martinez-Vicente, V., Topouzelis, K., 2020: Finding plastic patches in coastal waters using optical satellite data. Nature News. (on-line): https://www.nature.com/articles/s41598-020-62298-z .

Brown, C., Connor, L.N., Lillibridge, J., Nalli, N., Legeckis R., 2005: An introduction to satellite sensors, observations and techniques, ReseachGate, (on-line): (PDF) An introduction to satellite sensors, observations and techniques (researchgate.net) .

Brown, H., 2022: What is Plastic Made of and How is it Manufactured (on-line): https://nationwideplastics.net/plastic/what-is-plastic-made-of-and-how-is-it-manufactured.html .

C2RCC Community Project: Atmospheric Correction and In-water Processing of Optical Earth Observation Data [cit.2023.02.02], (on-line): C2RCC – The C2RCC Community web page .

Encyclopædia Britannica, inc. 2018: Spectrometer. Encyclopædia Britannica. (on-line): https://www.britannica.com/science/spectrometer .

ESRI Insider, 2016: What is orthorectified imagery? (on-line): What is orthorectified imagery? (esri.com) .

European Space Agency (ESA): Sentinel Online [cit.2023.02.01], (on-line): User Guides - Sentinel-2 MSI - Level-2A Product - Sentinel Online - Sentinel Online (esa.int) .

Freitas, S., Silva, H., Silva, E., 2021: Remote Hyperspectral Imaging Acquisition and Characterization for Marine Litter Detection. ResearchGate, (on-line): (PDF) Remote Hyperspectral Imaging Acquisition and Characterization for Marine Litter Detection (researchgate.net) .

GESAMP, 2019: Guidelines for the Monitoring and Assessment of Plastic Litter in the Ocean, Chapter 2, p. 5 - 11, (on-line): rs99e.pdf (oceanbestpractices.org) .

GIS Geography, 2022: Image classification techniques in remote sensing (on-line): https://gisgeography.com/image-classification-techniques-remote-sensing/ .

Guffogg, J., Blades, S., Soto-Berelov, M., Bellman, C. J., Skidmore, A. K., Jones, S. D., 2021: Quantifying marine plastic debris in a beach environment using spectral analysis. MDPI, (on-line): https://www.mdpi.com/2072-4292/13/22/4548 .

Gurjar, S. B., Padmanabhan, N., 2005: Study of various resampling techniques for high-resolution remote sensing imagery - journal of the Indian Society of Remote Sensing. SpringerLink., (on-line) https://link.springer.com/article/10.1007/BF02989999 .

Hu, C., 2009: A novel ocean color index to detect floating algae in the global oceans, Remote Sensing of Environment, Volume 113, Issue 10, Pages 2118-2129, ISSN 0034-4257, (on-line) https://doi.org/10.1016/j.rse.2009.05.012 .

Hu, C., Feng, L., Hardy, R., Hochberg, E., 2015: Spectral and spatial requirements of remote measurements of pelagic Sargassum macroalgae, Remote Sensing of Environment, Volume 167, Pages 229-246, ISSN 0034-4257, (on-line) https://doi.org/10.1016/j.rse.2015.05.022 .

Johnson, T., 2019: Just how important is plastic? ThoughtCo. (on-line): https://www.thoughtco.com/uses-of-plastics-820359 .

Kooi M., Reisser J., Slat B., Ferrari F. F., Schmid M. S., Cunsolo S., Brambini R., Noble K., Sirks L., Linders T., Schoeneicj-Agrent R. I., Koelmans A. A., 2016: The effect of particle properties on the depth profile of buoyant plastics in the ocean, Scientific Reports, (on-line): https://pame.is/document-library/desktop-study-on-marine-litter-library/additional-documents/683-kooi-2016-the-effect-of-particle-properties-on/file

Kou, L., Labrie, D., Chylek P., 1993: PubMed, Refractive indices of water and ice in the 0.65- to 2.5-µm spectral range. (on-line) https://pubmed.ncbi.nlm.nih.gov/20829977/ .

Laurencelle, J., 2022: What is sar? EARTHDATA. (on-line) https://asf.alaska.edu/information/sar-information/what-is-sar/ .

Malvern Panalytical, 2019: A newly designed leaf clip with smoother single-handed operation for the ASD range, (on-line): https://www.materials-talks.com/a-

newly-designed-leaf-clip-with-smoother-single-handed-operation-for-the-asd-range/ .

Moshtaghi, M., Knaeps, E., Sterckx, S., Garaba, S., Meire, D., 2021: Spectral reflectance of marine macroplastics in the VNIR and SWIR measured in a controlled environment. Nature News. (on-line): https://www.nature.com/articles/s41598-021-84867-6 .

Pereira-Sandoval, M., Ruescas, A., Urrego, P., Ruiz-Verdú, A., Delegido, J., Tenjo, C., Soria-Perpinyà, X., Vicente, E., Soria, J., & Moreno, J., 2019: Evaluation of atmospheric correction algorithms over Spanish inland waters for sentinel-2 multi spectral imagery data. MDPI (on-line): https://www.mdpi.com/2072-4292/11/12/1469 .

Piao ma, mu Wei Wang, Hui Liu, Yu Feng Chen & Jihong Xia., 2019: Research on ecotoxicology of microplastics on freshwater aquatic organisms, Environmental Pollutants and Bioavailability, 31:1, 131-137 (on-line): Research on ecotoxicology of microplastics on freshwater aquatic organisms (tandfonline.com) .

Price, C. 2019: Toxic ecosystems: The impact of plastic on Marine Life. Greenpeace USA. (on-line): https://www.greenpeace.org/usa/toxic-ecosystems-the-impact-of-plastic-on-marine-life/ .

Themistocleous, K., Papoutsa, C., Michaelides, S., & Hadjimitsis, D., 2020: Investigating detection of floating plastic litter from space using sentinel-2 imagery. MDPI. (on-line) https://www.mdpi.com/2072-4292/12/16/2648 .

Topouzelis, K., Papageorgiou, D., Karagaitanakis, A., Papakonstantinou, A., & Arias Ballesteros, M., 2020: Remote Sensing of sea surface artificial floating plastic targets with sentinel-2 and unmanned aerial systems (plastic litter project 2019). MDPI, (on-line) https://www.mdpi.com/2072-4292/12/12/2013 .

Topouzelis, K., Papakonstantinou, A., Shungudzemwoyo P. Garaba,. 2019: Detection of floating plastics from satellite and unmanned aerial systems (Plastic Litter Project 2018), International Journal of Applied Earth Observation and Geoinformation, Volume 79, Pages 175-183, ISSN 1569-8432, (on-line): https://doi.org/10.1016/j.jag.2019.03.011 .

Vanhellemont, Q., & Ruddick, K., 2021: Atmospheric correction of sentinel-3/olci data for mapping of suspended particulate matter and chlorophyll-a concentration in Belgian turbid coastal waters. Remote Sensing of Environment. (on-line): https://www.sciencedirect.com/science/article/pii/S003442572100002X .

Venrick, E. L., Backman, T. W., Bartram, W. C., Platt, C. J., Thornhill, M. S., Yates, R. E., 1973: Man-made objects on the surface of the central North Pacific Ocean. Nature News. (on-line): https://www.nature.com/articles/241271a0 .

Wageningen University & Research: Geographic Information Management and Applications (GIMA), Module 1 – Preprocessing, Chapter 5 p. 5-9, [cit.2023.02.02] (on-line): Remote Sensing: Overview, Basics and History (geo-informatie.nl) .

Wagner, M., Scherer, C., Alvarez-Muñoz, D., Brennholt, N., Bourrain, X., Buchinger, S., Fries, E., Grosbois, C., Klasmeier, J., Marti, T., Rodriguez-Mozaz, S., Urbatzka, R., Vethaak, A. D., Winther-Nielsen, M., & Reifferscheid, G., 2014: Microplastics in freshwater ecosystems: What we know and what we need to know. PubMed Central. (on-line): https://www.ncbi.nlm.nih.gov/pmc/articles/PMC5566174/ .

Wasser, L., 2023: About Hyperspectral remote Sensing Data, (on-line): About Hyperspectral Remote Sensing Data | NSF NEON | Open Data to Understand our Ecosystems (neonscience.org) .

Wright, S., Thompson, R., Galloway, T., 2013: The physical impacts of microplastics on marine organisms: A review, Environmental Pollution, Volume 178, Pages 483-492, ISSN 0269-7491, (on-line): https://www.sciencedirect.com/science/article/pii/S0269749113001140 .

11. Appendices

# Wavelength:													490	560	665	842
Name	X	Y	Lon	Lat	Label	PI	iop_adet	iop_agelb	iop_apig	iop_atot	iop_bpart	iop_bwit	rtoa_B2	rtoa_B3	rtoa_B4	rtoa_B8
pin_1	716.5	423.5	26.565523	39.107942	Plastic	0.4989474	0.0249077	0.182412	0.1015224	0.30884206	2.8756046	0.043830507	0.1375	0.0971	0.0714	0.0711
pin_2	717.5	423.5	26.565638	39.107943	Plastic	0.508502	0.1070288	0.2068564	0.0578074	0.37169263	1.6669923	0.102944456	0.1146	0.0893	0.0607	0.0628
pin_3	716.5	424.5	26.565523	39.107852	Plastic	0.4365482	0.2773317	0.2489347	0.030046	0.55631244	2.5854135	0.09379892	0.1151	0.0846	0.0666	0.0516
pin_4	717.5	424.5	26.565639	39.107853	Plastic	0.4659319	0.1223092	0.0961375	0.0103686	0.22881526	0.82457846	0.05970926	0.1036	0.0801	0.0533	0.0465
pin_5	719.5	419.5	26.565867	39.108304	Plastic	0.4423593	0.2331108	0.3574575	0.1470211	0.7375894	3.1192043	0.23963416	0.1179	0.089	0.0624	0.0495
pin_6	720.5	419.5	26.565983	39.108304	Plastic	0.4478958	0.1654181	0.181078	0.0272779	0.373774	1.1801285	0.06427765	0.1077	0.081	0.0551	0.0447
pin_7	719.5	420.5	26.565868	39.108214	Plastic	0.395102	0.6574563	0.2128731	0.146558	1.0168873	5.154509	1.1324059	0.1197	0.0858	0.0741	0.0484
pin_8	720.5	420.5	26.565984	39.108214	Plastic	0.4496982	0.0724551	0.1677356	0.0363627	0.27655336	1.491435	0.053580523	0.1113	0.086	0.0547	0.0447
pin_9	722.5	415.5	26.566212	39.108666	Plastic	0.5042333	0.0108515	0.0417074	0.0450834	0.09764237	0.98044837	0.008933093	0.1179	0.0814	0.0527	0.0536
pin_10	723.5	415.5	26.566328	39.108666	Plastic	0.4753927	0.0272892	0.0361274	0.0166511	0.080067664	0.68476874	0.053498942	0.1053	0.0756	0.0501	0.0454
pin_11	723.5	414.5	26.566327	39.108756	Plastic	0.466231	0.0572674	0.0349015	0.0067528	0.09892173	0.5475	0.10006246	0.1026	0.0746	0.049	0.0428
pin_12	722.5	414.5	26.566212	39.108756	Plastic	0.4930279	0.0294959	0.0634819	0.0260598	0.11903757	1.2572342	0.015170269	0.1135	0.083	0.0509	0.0495
pin_13	714.5	419.5	26.565289	39.108302	Shallow	0.4181286	0.4785065	0.4502133	0.3316709	1.2603908	2.7626562	0.6050444	0.1095	0.0937	0.0597	0.0429
pin_14	716.5	417.5	26.565519	39.108483	Shallow	0.4227642	0.3700621	0.1249534	0.0289306	0.5239461	4.293371	0.13397692	0.1077	0.088	0.0568	0.0416
pin_15	718.5	415.5	26.56575	39.108664	Shallow	0.4310521	0.311656	0.3730539	0.0924528	0.77716273	3.3303201	0.1665411	0.1084	0.0933	0.0557	0.0422
pin_16	725.5	423.5	26.566564	39.107946	Medium	0.4434994	0.0047258	0.0288312	0.0470764	0.080633424	0.38683003	0.018275812	0.1029	0.0719	0.0458	0.0365
pin_17	728.5	420.5	26.566909	39.108218	Medium	0.44	0.0037465	0.0334119	0.0541591	0.09131748	0.39128688	0.01217892	0.1054	0.0727	0.0462	0.0363
pin_18	723.5	426.5	26.566334	39.107675	Medium	0.4517705	0.0011688	0.0123832	0.0379293	0.05148134	0.29842788	0.00341282	0.1034	0.0703	0.0449	0.037
pin_19	745.5	430.5	26.568881	39.107324	Deep	0.4338139	0.0136103	0.0201236	0.0111814	0.044915326	0.25074294	0.07195641	0.0988	0.0661	0.0432	0.0331
pin_20	747.5	428.5	26.569111	39.107505	Deep	0.4298821	0.009742	0.0150863	0.0099482	0.034776617	0.19189876	0.055665456	0.0993	0.0653	0.0435	0.0328
pin_21	747.5	426.5	26.56911	39.107685	Deep	0.4239272	0.0187463	0.0224351	0.0094947	0.050676048	0.24435005	0.073902346	0.0989	0.0664	0.0443	0.0326
pin_1	397.5	275.5	33.045461	34.669601	Plastic	0.4023155	0.0288029	0.0651661	0.0185409	0.112509936	0.87186617	0.03492112	0.1188	0.0773	0.0413	0.0278
pin_2	398.5	275.5	33.04557	34.669601	Plastic	0.4110787	0.006254	0.0515468	0.0376484	0.09544909	0.5011968	0.016320871	0.1195	0.078	0.0404	0.0282
pin_3	397.5	274.5	33.045461	34.669691	Plastic	0.4008876	0.0953264	0.072082	0.0079079	0.17531627	0.9704125	0.05949497	0.1162	0.0773	0.0405	0.0271
pin_4	398.5	274.5	33.04557	34.669691	Plastic	0.4143885	0.0262774	0.0585374	0.0220324	0.106847204	0.9754188	0.02746179	0.1213	0.0781	0.0407	0.0288
pin_5	387.5	265.5	33.04437	34.670503	Shallow	0.3532847	0.1381103	0.0196062	0.002415	0.16013144	2.0358953	0.30905044	0.1245	0.0903	0.0443	0.0242
pin_6	390.5	258.5	33.044698	34.671134	Shallow	0.3592896	0.1547028	0.0378187	0.0024949	0.19501637	1.1408577	0.4839469	0.1239	0.0903	0.0469	0.0263
pin_7	394.5	254.5	33.045135	34.671495	Shallow	0.3362963	0.1549361	0.057315	0.0134135	0.22566454	2.3609998	0.51832306	0.1232	0.0886	0.0448	0.0227
pin_8	392.5	271.5	33.044915	34.669962	Medium	0.3673469	0.055125	0.0609215	0.013519	0.12956549	1.2692387	0.0492672	0.119	0.0797	0.0372	0.0216
pin_9	396.5	266.5	33.045352	34.670413	Medium	0.3813421	0.106353	0.0456324	0.0037773	0.15576267	0.99261487	0.14410765	0.1202	0.0782	0.0378	0.0233
pin_10	401.5	261.5	33.045898	34.670863	Medium	0.3684211	0.0993232	0.0419058	0.0034715	0.14470041	0.87413514	0.1434811	0.1166	0.0755	0.0372	0.0217
pin_11	403.5	281.5	33.046116	34.66906	Deep	0.3405797	0.0607615	0.0179281	0.0013405	0.080030076	0.34545586	0.2759942	0.1073	0.0683	0.0364	0.0188
pin_12	407.5	276.5	33.046552	34.66951	Deep	0.3474264	0.0769979	0.0368512	0.0031912	0.11704027	0.5566957	0.16865031	0.1089	0.0687	0.0355	0.0189
pin_13	411.5	270.5	33.046989	34.670051	Deep	0.3646409	0.05046	0.0580648	0.0099548	0.11847957	0.87777674	0.073439404	0.1115	0.0717	0.0345	0.0198
pin_1	397.5	165.5	26.566099	39.108215	Plastic	0.43531	0.0016678	0.0216392	0.0423808	0.065687746	0.3317389	0.005284325	0.1072	0.0711	0.0419	0.0323
pin_2	398.5	165.5	26.566215	39.108215	Plastic	0.4733994	0.1113972	0.2816541	0.098785	0.4918363	1.1659256	0.12351027	0.1156	0.0803	0.0584	0.0525
pin_3	399.5	165.5	26.566331	39.108216	Plastic	0.457971	0.2666994	0.2454926	0.0565112	0.5687033	3.0170019	0.2405581	0.1145	0.0826	0.0561	0.0474
pin_4	397.5	166.5	26.5661	39.108125	Plastic	0.4693877	0.001752	0.0223407	0.0426416	0.066734344	0.32508183	0.005586254	0.1082	0.0716	0.0442	0.0391
pin_5	398.5	166.5	26.566215	39.108125	Plastic	0.4591837	0.0046892	0.0508863	0.0522091	0.107784525	0.499036	0.008729467	0.1189	0.0785	0.053	0.045
pin_6	399.5	166.5	26.566331	39.108125	Plastic	0.4321839	0.1257791	0.073966	0.0073123	0.20705737	1.2005115	0.1155042	0.1118	0.0767	0.0494	0.0376
pin_7	391.5	164.5	26.565405	39.108302	Shallow	0.3928144	0.1786755	0.3059927	0.1282461	0.6129144	1.9089696	0.2174184	0.1117	0.0869	0.0507	0.0328
pin_8	393.5	162.5	26.565635	39.108483	Shallow	0.3880239	0.1219922	0.3670969	0.1675897	0.6566788	2.2710156	0.20154598	0.1119	0.0884	0.0511	0.0324
pin_9	395.5	160.5	26.565865	39.108664	Shallow	0.3994975	0.0551869	0.1963565	0.0602653	0.31180862	1.3117251	0.07751749	0.1092	0.0839	0.0478	0.0318
pin_10	401.5	172.5	26.566566	39.107586	Medium	0.4029851	0.0083891	0.0158326	0.0119468	0.03616845	0.19680291	0.03039002	0.1043	0.0672	0.04	0.027
pin_11	404.5	170.5	26.566912	39.107767	Medium	0.4	0.004196	0.0282458	0.0387117	0.07115354	0.30105945	0.019613946	0.1055	0.0699	0.0393	0.0262
pin_12	407.5	167.5	26.567257	39.108039	Medium	0.3942598	0.0092319	0.0290155	0.0183977	0.056645073	0.2710883	0.06504754	0.1039	0.0677	0.0401	0.0261
pin_13	421.5	190.5	26.568889	39.105972	Deep	0.3918495	0.0130429	0.0224561	0.0100138	0.04551275	0.18619774	0.06020225	0.101	0.0651	0.0388	0.025
pin_14	427.5	184.5	26.569579	39.106515	Deep	0.3681592	0.0092586	0.0109391	0.0093093	0.029506993	0.1384844	0.038718082	0.1016	0.0637	0.0381	0.0222
pin_15	435.5	176.5	26.5705	39.10724	Deep	0.3783333	0.0103172	0.0202382	0.0107851	0.041340493	0.20916644	0.0643775	0.102	0.0635	0.0373	0.0227
pin_1	491.5	284.5	26.565638	39.108033	Plastic	0.4713604	0.0092106	0.0337415	0.0302549	0.073206924	0.42000225	0.044488378	0.1015	0.0705	0.0443	0.0395
pin_2	491.5	285.5	26.565638	39.107943	Plastic	0.4725877	0.0902527	0.1084426	0.0123363	0.21103169	0.9565179	0.05769256	0.1064	0.0748	0.0481	0.0431
pin_3	490.5	285.5	26.565523	39.107942	Plastic	0.4322581	0.0312182	0.0253086	0.0073364	0.06386317	0.27453473	0.088560484	0.0974	0.0683	0.044	0.0335
pin_4	490.5	284.5	26.565522	39.108032	Plastic	0.4248705	0.0421698	0.0206535	0.0062774	0.069100596	0.21748339	0.0560073	0.0976	0.0684	0.0444	0.0328
pin_5	495.5	286.5	26.566101	39.107854	Plastic	0.4091521	0.0441379	0.0843185	0.0137685	0.14222491	0.6972129	0.059801355	0.1023	0.0706	0.0439	0.0304
pin_6	496.5	286.5	26.566217	39.107855	Plastic	0.4231242	0.1492685	0.1163275	0.0108348	0.27643082	0.8966576	0.081024386	0.1056	0.0724	0.0469	0.0344
pin_7	497.5	286.5	26.566333	39.107855	Plastic	0.4278215	0.0100632	0.0367539	0.0270713	0.073888406	0.40144253	0.052053835	0.1028	0.0686	0.0436	0.0326
pin_8	496.5	287.5	26.566218	39.107765	Plastic	0.4152431	0.0683461	0.0800206	0.0099091	0.15827577	0.5672531	0.07550806	0.1009	0.0702	0.0445	0.0316
pin_9	495.5	281.5	26.566099	39.108305	Plastic	0.4202335	0.0279468	0.0274941	0.0108135	0.06625432	0.17714112	0.047091432	0.0971	0.0675	0.0447	0.0324
pin_10	496.5	281.5	26.566214	39.108305	Plastic	0.4529817	0.0082598	0.0673328	0.0394603	0.11505289	0.5168518	0.00969447	0.1062	0.0736	0.0477	0.0395
pin_11	495.5	280.5	26.566098	39.108395	Plastic	0.4224966	0.0109656	0.0168461	0.0108704	0.038682107	0.1738738	0.04919289	0.0953	0.066	0.0421	0.0308
pin_12	496.5	280.5	26.566214	39.108395	Plastic	0.4298821	0.0060314	0.0177151	0.0180676	0.04181411	0.23694539	0.03529291	0.1021	0.0671	0.0435	0.0328
pin_13	500.5	281.5	26.566677	39.108307	Plastic	0.4296875	0.0114542	0.0533712	0.0299327	0.09475816	0.5303939	0.033751566	0.1044	0.0705	0.0438	0.033
pin_14	501.5	281.5	26.566793	39.108307	Plastic	0.421671	0.0069874	0.0520197	0.0431148	0.10212189	0.5390277	0.016567975	0.1081	0.0719	0.0443	0.0323
pin_15	502.5	281.5	26.566908	39.108308	Plastic	0.4289655	0.0022778	0.026236	0.0549441	0.083457924	0.3656738	0.007756168	0.1033	0.07	0.0414	0.0311
pin_16	500.5	280.5	26.566676	39.108397	Plastic	0.4474761	0.002164	0.0208198	0.0494777	0.07246146	0.34925732	0.007810735	0.1013	0.0682	0.0405	0.0328
pin_17	501.5	280.5	26.566792	39.108397	Plastic	0.4213264	0.0142027	0.0581355	0.0260598	0.09839804	0.5540111	0.03813724	0.1053	0.0704	0.0445	0.0324
pin_18	499.5	279.5	26.56656	39.108487	Plastic	0.4368557	0.1130457	0.0710297	0.008838	0.19291332	0.5312514	0.06051264	0.0979	0.0681	0.0437	0.0339
pin_19	499.5	278.5	26.56656	39.108577	Plastic	0.4589744	0.0091311	0.0441592	0.0311233	0.084413595	0.43558472	0.039174683	0.1021	0.0688	0.0422	0.0358
pin_20	498.5	278.5	26.566444	39.108576	Plastic	0.4456522	0.0061556	0.0209774	0.0263762	0.053509153	0.28466752	0.04372193	0.099	0.0656	0.0408	0.0328
pin_21	497.5	287.5	26.566333	39.107765	Plastic	0.4199193	0.0045888	0.0197836	0.0303884	0.05476078	0.2787891	0.027859243	0.1026	0.0676	0.0431	0.0312
pin_22	503.5	277.5	26.567022	39.108669	Plastic	0.4518614	0.0044635	0.0278232	0.0400736	0.07236023	0.32472572	0.02545501	0.1032	0.0684	0.0427	0.0352
pin_23	504.5	277.5	26.567137	39.108669	Plastic	0.4554707	0.0294959	0.0575251	0.0133872	0.10040814	0.47199687	0.079459056	0.0995	0.069	0.0428	0.0358
pin_24	503.5	276.5	26.567021	39.108759	Plastic	0.4268456	0.0169039	0.0157109	0.0100204	0.04263521	0.15133928	0.045022678	0.0982	0.0657	0.0427	0.0318
pin_25	504.5	276.5	26.567137	39.108759	Plastic	0.4295393	0.024391	0.0282974	0.0092848	0.06197322	0.23474233	0.073477864	0.0973	0.0665	0.0421	0.0317
pin_26	491.5	277.5	26.565634	39.108664	Shallow	0.3879222	0.3576723	0.4272849	0.4348283	1.2197855	7.864617	0.9433068	0.115	0.0993	0.0598	0.0379
pin_27	488.5	280.5	26.565289	39.108392	Shallow	0.3895411	0.466494	0.4139225	0.2790526	1.1594691	3.7637677	0.8002744	0.1096	0.0946	0.0572	0.0365
pin_28	486.5	282.5	26.565058	39.108211	Shallow	0.3888889	0.7991677	0.1327414	0.0967604	1.0286695	4.3036737	1.4444163	0.1082	0.0909	0.0572	0.0364
pin_29	505.5	287.5	26.567259	39.107768	Medium	0.4252078	0.0067525	0.0235738	0.0259937	0.05631992	0.2922685	0.048995342	0.1007	0.066	0.0415	0.0307
pin_30	508.5	284.5	26.567604	39.10804	Medium	0.4289773	0.0041251	0.0230949	0.0363853	0.06360532	0.2976102	0.024136448	0.0999	0.0672	0.0402	0.0302
pin_31	511.5	281.5	26.567949	39.108312	Medium	0.4376731	0.0056302	0.0493373	0.0496276	0.104595125	0.5495638	0.01248486	0.1056	0.0709	0.0406	0.0316
pin_32	516.5	292.5	26.568534	39.107323	Deep	0.4151213	0.063846	0.0393016	0.0176858	0.12083343	0.16211653	0.026381377	0.0973	0.0637	0.041	0.0291
pin_33	520.5	287.5	26.568993	39.107775	Deep	0.4160584	0.0257479	0.0281685	0.0082427	0.062159095	0.20608857	0.07937537	0.0983	0.0627	0.04	0.0285
pin_34	525.5	280.5	26.569568	39.108408	Deep	0.4300442	0.0111261	0.0232138	0.0123202	0.04666006	0.22231495	0.066479556	0.0985	0.0625	0.0387	0.0292
pin_1	382.5	187.5	26.565987	39.107674	Plastic	0.4343708	0.0411465	0.1966771	0.0818629	0.31968653	1.8811909	0.045564193	0.1004	0.0842	0.0418	0.0321
pin_2	381.5	187.5	26.565871	39.107673	Plastic	0.478673	0.0603226	0.1338539	0.0273992	0.22157574	1.447455	0.032210525	0.1093	0.0735	0.044	0.0404
pin_3	381.5	186.5	26.565871	39.107763	Plastic	0.4434561	0.1406692	0.0950758	0.017413	0.253158	0.7995186	0.03154515	0.101	0.0658	0.0438	0.0349
pin_4	382.5	186.5	26.565986	39.107764	Plastic	0.4190871	0.0968145	0.1422505	0.0165434	0.25560844	0.953564	0.051399525	0.0987	0.0705	0.042	0.0303
pin_5	383.5	183.5	26.5661	39.108034	Plastic	0.5363735	0.0055703	0.0118846	0.0131445	0.03059939	0.2261336	0.03335052	0.1037	0.0635	0.0427	0.0494
pin_6	384.5	183.5	26.566216	39.108035	Plastic	0.544	0.6593409	0.2824636	0.2176701	1.1594747	4.9765806	1.7600375	0.109	0.0889	0.0741	0.0884
pin_7	384.5	182.5	26.566215	39.108125	Plastic	0.4515418	0.4694767	0.4149203	0.0930803	0.97747725	3.2726865	0.117199875	0.0943	0.0736	0.0498	0.041
pin_8	383.5	182.5	26.5661	39.108125	Plastic	0.4639456	0.0083939	0.04354	0.0364758	0.08840969	0.48206636	0.02767892	0.0989	0.0675	0.0394	0.0341
pin_9	383.5	179.5	26.566098	39.108395	Plastic	0.4363104	0.0929079	0.0888802	0.0089609	0.19074896	0.7924287	0.08389956	0.0979	0.0675	0.0385	0.0298
pin_10	383.5	178.5	26.566098	39.108485	Plastic	0.4296296	0.1417473	0.1136836	0.011441	0.266872	1.2126465	0.08702289	0.1	0.0709	0.0385	0.029
pin_11	382.5	178.5	26.565982	39.108485	Plastic	0.4119403	0.1620748	0.1371832	0.048882	0.34813994	2.8907692	0.15511817	0.1024	0.0752	0.0394	0.0276
pin_12	383.5	186.5	26.566102	39.107764	Plastic	0.4255319	0.0091417	0.0522791	0.0327658	0.09418655	0.4571447	0.030133735	0.0969	0.0667	0.0378	0.028
pin_13	375.5	181.5	26.565174	39.108211	Shallow	0.371367	0.7715185	0.1396366	0.0655399	0.97669494	4.262572	0.9860584	0.1079	0.0913	0.0584	0.0345
pin_14	377.5	179.5	26.565404	39.108392	Shallow	0.3748488	0.193936	0.0872654	0.024112	0.30531335	1.6327373	0.019914744	0.1025	0.0843	0.0517	0.031
pin_15	380.5	176.5	26.56575	39.108664	Shallow	0.3616751	0.4272038	0.2768748	0.1973304	0.901409	6.208816	0.9031755	0.105	0.0862	0.0503	0.0285
pin_16	390.5	195.5	26.566917	39.106956	Medium	0.4375	0.0041707	0.0298982	0.0430356	0.07710449	0.31716177	0.021552617	0.1013	0.0683	0.0414	0.0322
pin_17	396.5	187.5	26.567606	39.10768	Medium	0.4304124	0.0128018	0.0384027	0.0190508	0.07025528	0.3376039	0.06531768	0.1025	0.0683	0.0442	0.0334
pin_18	402.5	179.5	26.568296	39.108403	Medium	0.4302177	0.0123475	0.048987	0.0282979	0.089632325	0.518247	0.037023026	0.104	0.0719	0.0445	0.0336
pin_19	406.5	207.5	26.568774	39.105882	Deep	0.4265823	0.0513798	0.0348396	0.0059363	0.09215578	0.34526685	0.110748865	0.1028	0.069	0.0453	0.0337
pin_20	415.5	191.5	26.569806	39.107327	Deep	0.4166667	0.0290041	0.0174126	0.0066339	0.053050593	0.17207484	0.05861618	0.1042	0.0685	0.0476	0.034
pin_21	427.5	174.5	26.571184	39.108864	Deep	0.4392857	0.0108705	0.0084106	0.006224	0.025504993	0.12814027	0.06535154	0.105	0.0683	0.0471	0.0369

***Table 11.1**: Table of values extracted from pins placed on plastic targets, as well as shallow, medium, and deep water from five remote sensing images (Dec 15, 2018, June 07, 2018, Apr 18, 2019, May 03, 2019, June 07, 2019) With PI, iop_adet, iop_agelb, iop_apig, iop_atot, iop_bpart, iop_bwit, being : Plastic Index, Absorption coefficient of detritus, Absorption coefficient of gelbstoff, Absorption coefficient of phytoplankton pigments, Phytoplankton + detritus + gelbstoff absorption, Scattering coefficient of marine particles, Scattering coefficient of white particles respectively.*

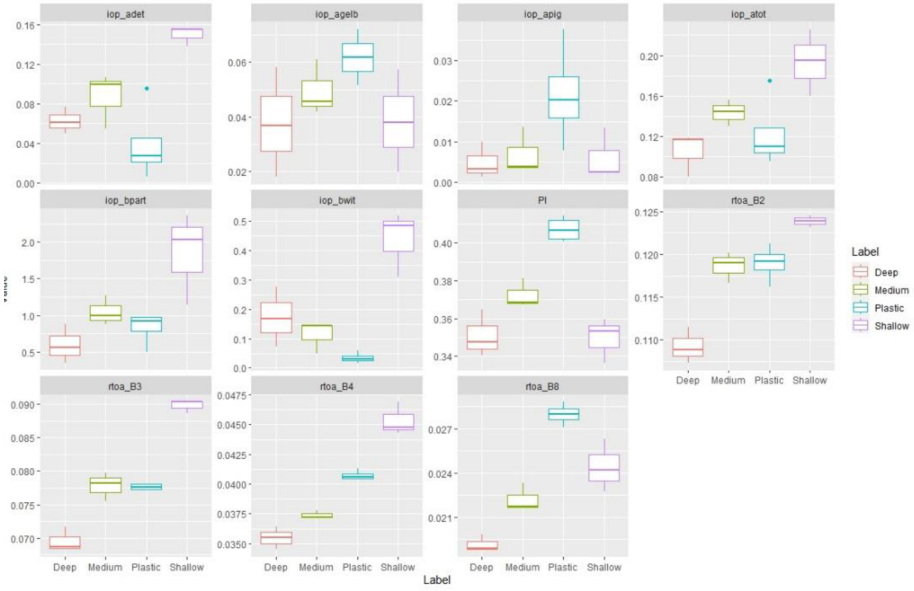

***Figure 11.2**: Distribution of values for individual bands and indices from Sentinel-2 image acquired on December 15, 2018*

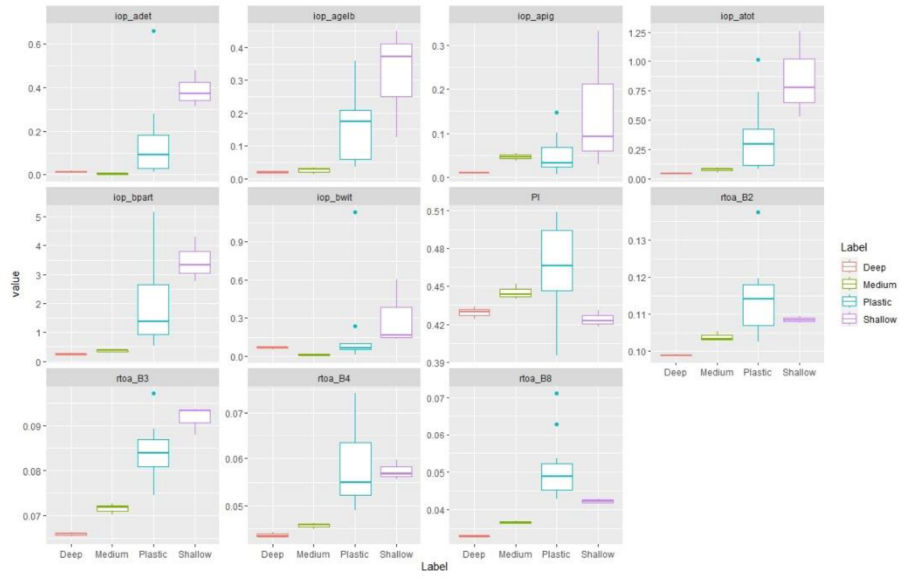

***Figure 11.3**: Distribution of values for individual bands and indices from Sentinel-2 image acquired on June 07, 2018*

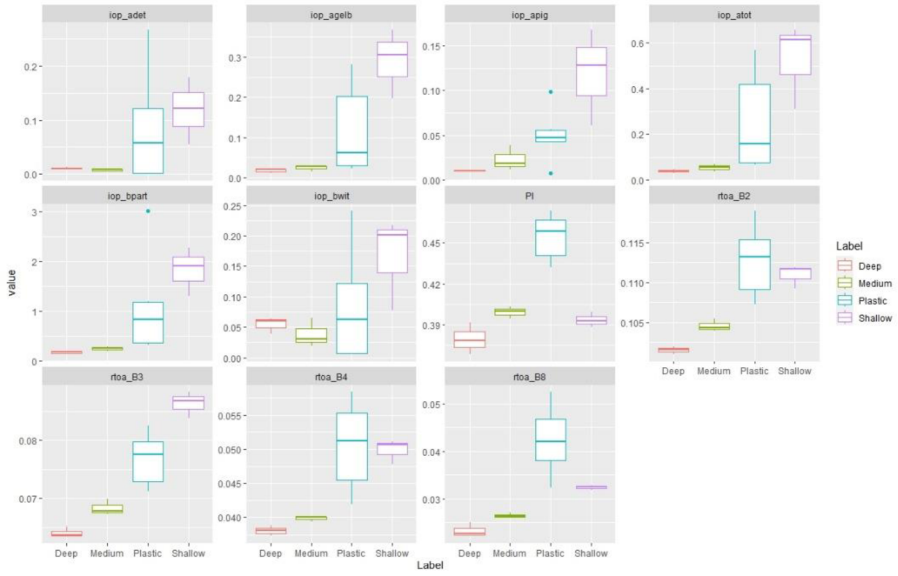

***Figure 11.4**: Distribution of values for individual bands and indices from Sentinel-2 image acquired on April, 18, 2019*

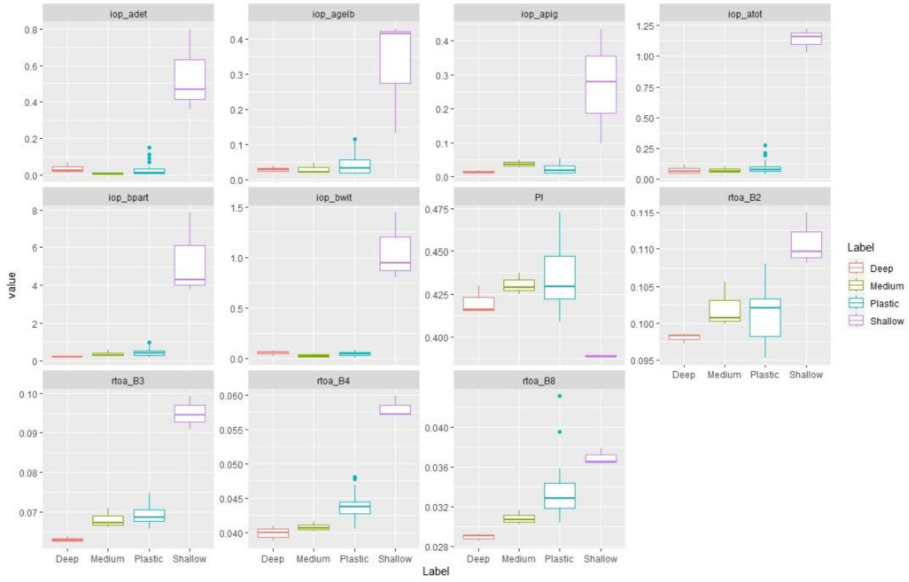

***Figure 11.5**: Distribution of values for individual bands and indices from Sentinel-2 image acquired on May, 03, 2019*

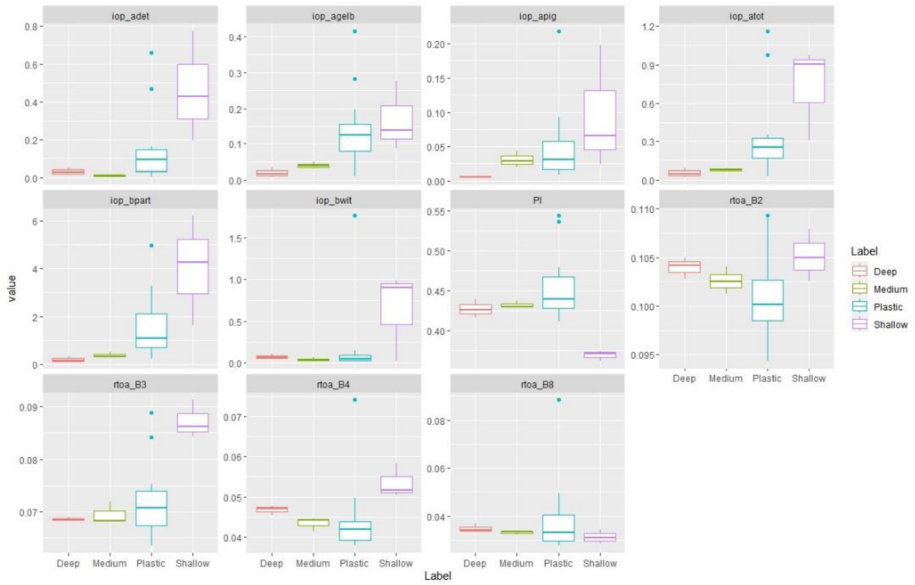

***Figure 11.6**: Distribution of values for individual bands and indices from Sentinel-2 image acquired on June 07, 2019*

```
## importing data of pixels containing reflectance values

> library(readxl)
> Pins_ALL <- read_excel("E:/CZU/THESIS/data all plastic targets/Pins
ALL.xlsx",
+     skip = 6)
> View(Pins_ALL)
> Pins_ALL$Label <- factor(Pins_ALL$Label)
> summary(Pins_ALL)


## visualizing data distribution using boxplots

> Pins_ALL %>%
+ pivot_longer(8:18)%>%
+ ggplot(aes(x=Label,y=value,col=Label))+
+ geom_boxplot()+
+ facet_wrap(~name, scales="free_y")

## statistical analysis using Random Forest algorithm

library(ranger)

> mr <- ranger(Label~ PI + iop_adet + iop_agelb + iop_bpart + rtoaB2 +
rtoa_B3 + rtoa_B4 + rtoa_B8, data = Pins_ALL, importance = "impurity")
> importance(mr)/sum(importance(mr))

> library(caret)

> confusionMatrix(predictions(mr), Pins_ALL$Label)
```

***Figure 11.7**: Full code used in "R Studio" statistical software to visualize plastic reflectance data using boxplots, and test the Random Forest algorithm. *Pins_ALL being the file containing the pixel values from the remotely sensed images (refer to Table 11.1 of this section)*